Spotlight

A Novel Constant Directivity Horn

By Dario Cinanni

Editor's Note: This outstanding article on constant directivity horn design is profusely illustrated with 45 images and graphs, which unfortunately will not fit into the available print space for this issue of Voice Coil *magazine. The additional figures (marked in blue) as well as the complete article can be viewed here:* http://bit.ly/Cinanni

This article was written based on an acoustic simulation study I presented at the Comsol Conference, Grenoble (France) in October 2015 (www.comsol.com/paper/simulation-of-horn-driver-response-by-direct-combination-of-cd-frequency-respons-28561). In that research, a new simulation method was presented about high-frequency horn driver transducers. The method comprises a horn simulation and a driver plane wave tube measurement.

Combining only this data, using a novel equation that correlates the matrix of the virtual horn and the real compression driver pressure, it is possible to easily predict the absolute sound pressure level (SPL) of the real horn driver frequency response. The results showed a good match between simulations and measurements up to 15 kHz. We found that the main limit is the assumption of a plane wave, which does not hold for higher frequencies. In order to easily understand the content of this article, in particular for audio and acoustic aficionados approaching these topics for the first time, I have left out the mathematic formulas, for which a deeper and distinct analysis would be necessary.

Hybrid Constant Directivity

The two main reasons why horns are used in sound systems are high efficiency (and consequently high SPL at relatively low distortion) and directivity control. We want to focus on the second point: directivity, as discussed by Bjørn Kolbrek ("Horn Theory: An Introduction Part 1 and Part 2, *audioXpress,* March and April, 2008): an exponential horn can provide the driver with uniform loading, but at high frequencies, it starts to beam. Constant directivity horns, if based on conical shapes only or diffraction methods, are affected by reflecting waves that at high levels could produce distortions. The question is: Is it possible to transform a conventional expansion horn (exponential, hyperbolic sine, hyperbolic cosine, catenoidal, tractrix, spherical, etc.) into a constant directivity horn?

We need to consider a mathematical expansion law of a horn not only as an expansion in terms of an area, but also in terms of a volume. If we keep the defined horn expansion law following the same volume expansion, within certain limits, we can modify boundary profiles to satisfy special needs. The need we want to satisfy is the constant directivity. As we know, the directivity of a horn is controlled down to a frequency that has a wavelength comparable to the horn mouth.

Horn.ell.a is software designed in 2006 and its algorithm doesn't follow Cartesian profiles, as per the usual approach with a horn, but it works on volumes. With the volume process, it is possible to extend expansion profiles for a progressive match between the throat and the different mouth shapes.

The horn's mathematical progression is always guaranteed, so the key is to have a non-deformable volume gradient. In this way, if we want a hyperbolic exponential profile, we will maintain the same load and low-frequency control, but we can also obtain the directivity control on one plane.

The volume expansion is discretized by the X, Y, value numbers. As for the 2D mathematical profile, the 3D volume discretization approximates the selected ideal expansion. Better approximation occurs when reducing the step as it is observable in **Figure 1**. For the current prototypes, on the X-axis for example, an X value is carefully selected to obtain a step of 1.85 mm, thus every 1.85 mm the horn volume adapts its expansion matching the selected mathematical law. This is a coarse step, generating a 61k point's cloud—useful for a demonstration purpose—but for an accurate surface reconstruction of a similar product with this dimension, a finer mesh is suggested—about 1M points.

We can call these new kinds of horns Hybrid Constant Directivity (HCD) and they can guarantee:

- the expansion we already know
- a constant directivity on the plane along its major axis
- an equivalent directivity contour we have with a circular mouth horn (using the same expansion) on the plane along its minor axis

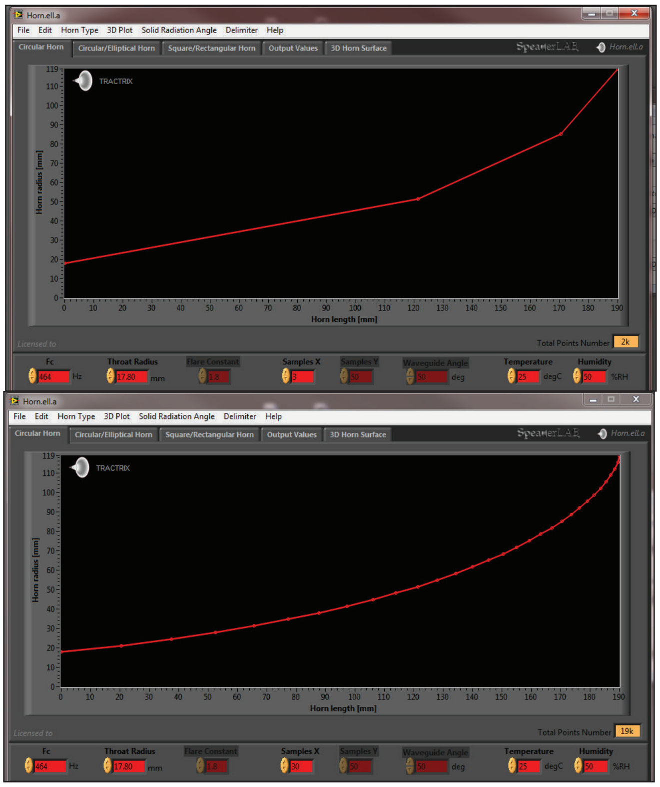

Total Points Number 2k

Fc 464 Hz
Throat Radius 17.80 mm
Flare Constant 1.8
Samples X 3
Samples Y 50
Waveguide Angle 50 deg
Temperature 25 degC
Humidity 50 %RH

Total Points Number 19k

Fc 464 Hz
Throat Radius 17.80 mm
Flare Constant 1.8
Samples X 30
Samples Y 50
Waveguide Angle 50 deg
Temperature 25 degC
Humidity 50 %RH

Figure 1: Sample X represents the segments number that approximates the horn volume expansion on the X-axis. X = 3 (left), X = 30 (right).

With this type of horns, the maintenance of constant directivity with frequency in high-frequency exponential horns (and all other expansions) is possible on one plane. A horn with a good loading but a constant directivity (e.g., the HCD horns) is the most natural way to do it. These horns are useful for all applications where directivity control on one plane is requested. On the other plane, the directivity behavior will be similar to a standard circular horn. Various HCD horns are now available on the market, mainly from the Italian professional audio manufacturer as single components and used all over the world in diverse loudspeaker systems.

Aspect-Ratio

First, we are going to analyze a commercial 1.4" throat elliptical mouth horn (see **Figure 2**), which was designed using Horn.ell.a software. We can use constant directivity along a vertical line or along a horizontal line; it depends on requirements and by the application. For this reason, to avoid confusion, I prefer to discuss general planes and not vertical or horizontal ones. For convenience, we define two section planes. A is the section along the major axis of the horn mouth (the plane A here is always referred to the constant directivity section plane); while B is the one along the minor axis. This is true when the horn mouth has an aspect-ratio greater than 1. The "mouth aspect-ratio" (MR) is always referred to the horn mouth and it represents the ratio between mouth major and minor axis (see **Figure 3**).

Usually ratios between values of 1 and 1.8 are used. If the aspect-ratio = 1, the horn has a circular or square mouth and we have only one section plane (because Plane A = Plane B). Horn.ell.a version 2.0 uses a new routine allowing the user to have aspect-ratios greater than 2,

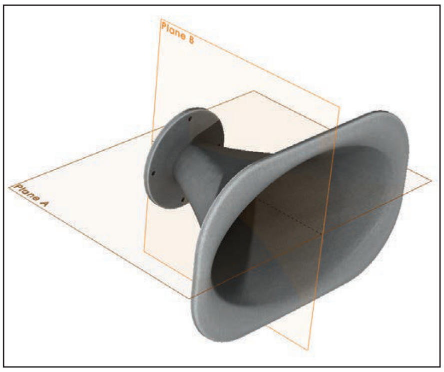

Figure 2: Section planes—Plane A is along the major axis of the horn mouth. Plane B is along the minor axis.

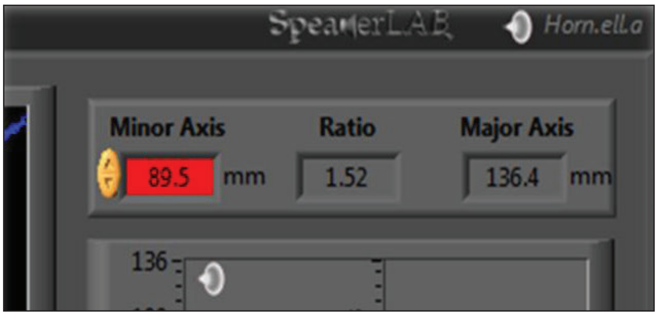

Minor Axis 89.5 mm
Ratio 1.52
Major Axis 136.4 mm
136

Figure 3: The horn mouth aspect-ratio is the ratio between mouth's major axis and minor axis.

maintaining the selected mathematical expansion and reducing wave-front deformations. Modifying the mouth ratio of a horn, Horn.ell.a changes the major and the minor axes, gradually transforming the major axis in a pseudo-conical profile, obtaining an accurate constant directivity on one plane. On the other section plane, the mathematical progression is analogous to the selected one (hyperbolic, tractrix, spherical, etc.).

Next, we will see how it is possible to increase the aspect-ratio, discover how the aspect-ratio value is linked to the constant directivity coverage angle, and determine why the aspect-ratio value is being increased.

Horn Driver Standard Model

A rigid circular piston (with a planar surface and the same radius of the horn throat) has been modeled as a source to load all the simulated horns. This condition produces an acoustic pressure, in order to predict the horns' directivity. The standard model generates directivity as seen in **Figure 4** and **Figure 5**.

Analyzing the results, starting from a certain frequency the simulated high-frequency band, as we can see from the Figure 4 and Figure 5 contours and is different compared to the measurements graphs shown in **Figure 6** and **Figure 7**.

The scope is trying to study in detail the horn driver high-frequency directivity behavior, in order to improve the simulation results and also to calibrate the model. This step is necessary if we want to predict the horns' directivity plots with a good accuracy. The measurements were done using a compression driver mounted to the real horn as shown in Figure 2; together they produce a frequency response (see **Figure 8**).

If we put the compression driver phase-plug design into the simulated model, we can see that the simulations of **Figure 9** and **Figure 10** and the measurements of **Figure 11** and **Figure 12** are similar, with an improved match at higher frequencies.

This is due to phase-plug acoustic expansion on its channels exit. Consequently, starting at a certain frequency, which depends on the horn throat diameter, the higher frequency directivity depends more on geometry, shape, channel number, and mathematical progression of the phase-plug.

Simulation accuracy is obtained when we model the full horn driver, with the entire compression driver, because the systems are strongly coupled, hence they can't be decoupled. However, with some smart ideas we can reduce the error to an acceptable level. My target is to have a general and valid horn model independent of the compression driver, but high frequencies will always be a challenge.

Considering the chromatic match between simulations and measurements of the directivity color plots, in the next graphs (**Figure 13** and **Figure 14**), we can appreciate a numerical match of the beam-width. Beam-width is defined here as the coverage angle in which an SPL loss of 6 dB occurs relative to the zero degrees reference angle (the on-axis direction).

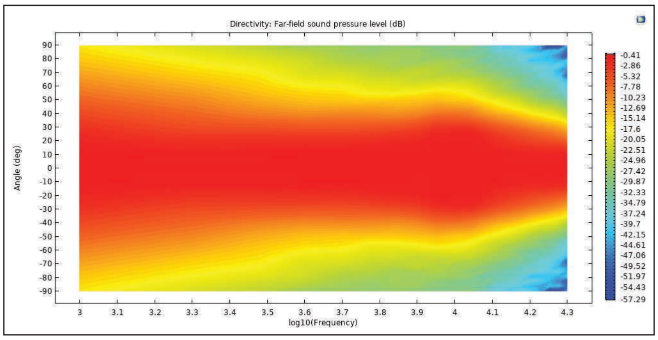

Figure 4: Simulated Plane A directivity plot

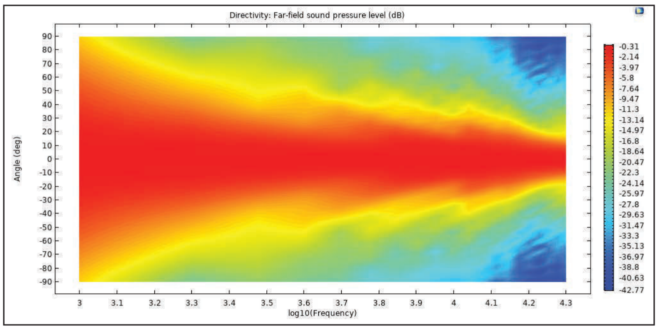

Figure 5: Simulated Plane B directivity plot

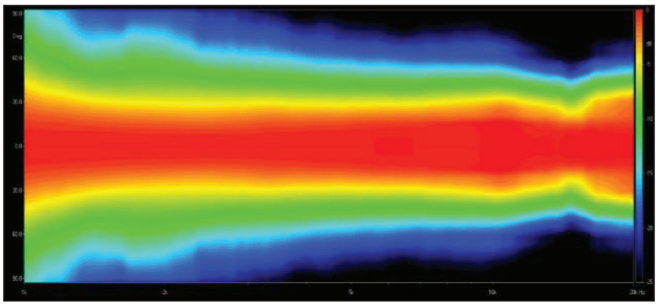

Figure 6: Measured Plane A directivity plot (smooth 1/2 octave)

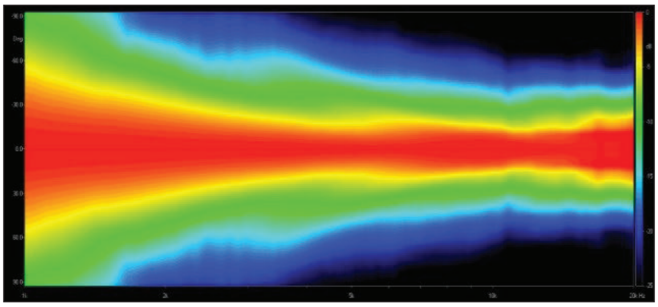

Figure 7: Measured Plane B directivity plot (smooth 1/2 octave)

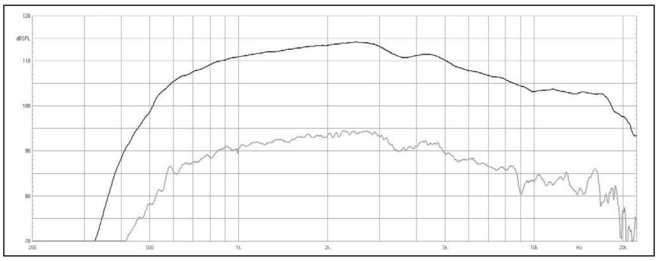

Figure 8: The horn driver is shown at 1 W frequency response. The microphone is set at 1 m distance from the mouth axis. The measurement was taken in anechoic room in a free-field condition. The upper curve is a smooth 1/3 octave, the lower curve -20 dB unsmoothed frequency response.

PUNKTKILDE™

Designed by Scan-Speak Transducers

"Dual-Suspensions" Series of Transducers

From 2" up to 5.25", using our patented Dual-Suspensions design; breaking the rules on traditional suspension transducers, to deliver high excursions and extremely low distortion. With this innovation on transducers design, now you can design small, compact systems without compromising performance.

Magnesium-Lithium Alloy Cone Series of Transducers

PUNKTKILDE has developed a series of transducers utilizing Magnesium-Lithium (Mg-Li) Alloy cone material, from 1" Dome Tweeters up to 8" Woofers. This unique alloy material has good damping properties, low cone density, high stiffness, and low moving mass, delivering good pistonic behavior and fast transient response.

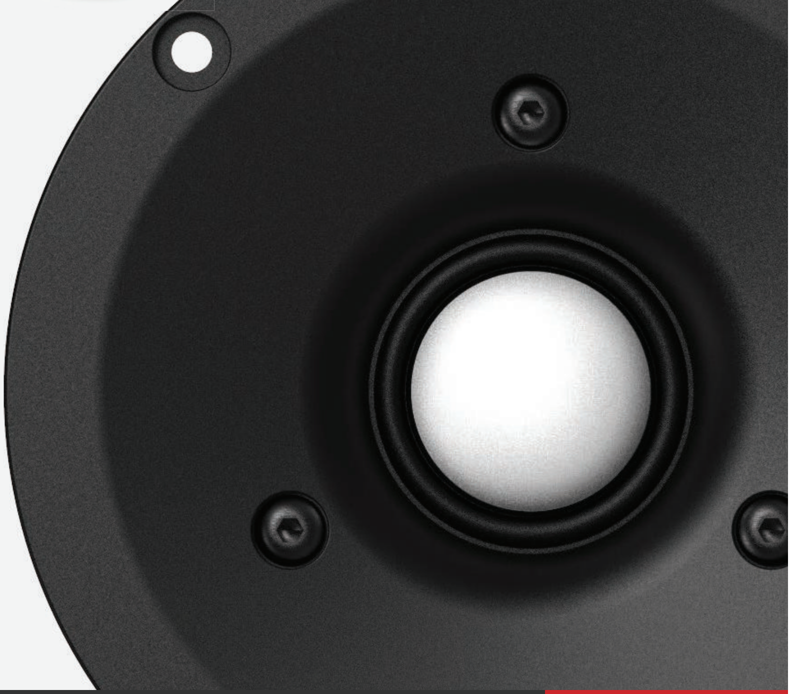

E marketing@eastech.com

Proudly produced by EASTECH

W www.punktkilde.com

As we can see in Figure 13, on Plane A the beam-width is well controlled, in this case we see a coverage angle of 62.3° in the frequency range 1.35÷20 kHz. On Plane B (Figure 14) from 4 kHz upward there is a regular beam-width, but it exceeds 6 dB, moreover it is not fixed but it depends on the selected expansion. So for the Plane B, we can calculate an average value but in my opinion it is not formally correct to give a unique value because the reader, or a buyer of a similar product, could be misled when comparing HCD to CD horns. This rule is also valid for all cases of horns with a non-constant directivity beam-width (e.g., all pure profiles such as exponential, tractrix, spherical, etc. with a circular mouth). It doesn't make sense to declare a coverage angle with a single value in a similar situation because we can use them, but these horns in pure shapes were not designed for this purpose. For HCD horns, we can use, for example, the wording "coverage angle x selected expansion," so the Figure 2 horn could be a commercial 60° x Hyperbolic. For that reason, I introduced the name "Hybrid" constant directivity horn.

We also need to consider, for a better organization of this work that between 1 kHz and 2 kHz there are no other simulated points, as we see in Figure 13 a straight line between these two frequencies. From the beam-width analysis, we can see that it is possible to improve the model simply by adding a phase-plug. Up to 15 kHz the simplified model works well for our purposes, because you must always take into account that a different phase-plug (so a different compression driver!) will influence the upper frequency range. Therefore, we can work with 3D horn simulations only—considering the model's reliability—paying attention to all next directivity and beam-width plots and not considering the high frequency (>15 kHz) beam, because as we have previously seen in real conditions, the directivity depends on the horn-driver combination.

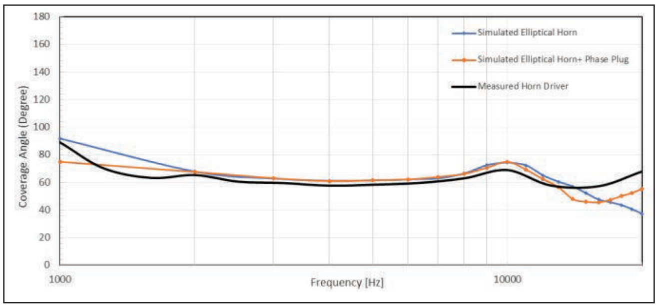

Figure 13: Beam-width measurement and simulations on Plane A

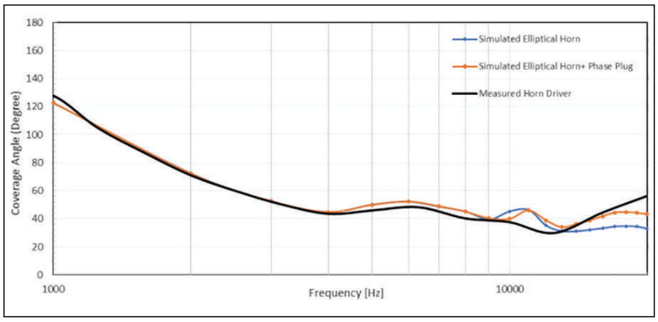

Figure 14: Beam-width measurement and simulations on Plane B

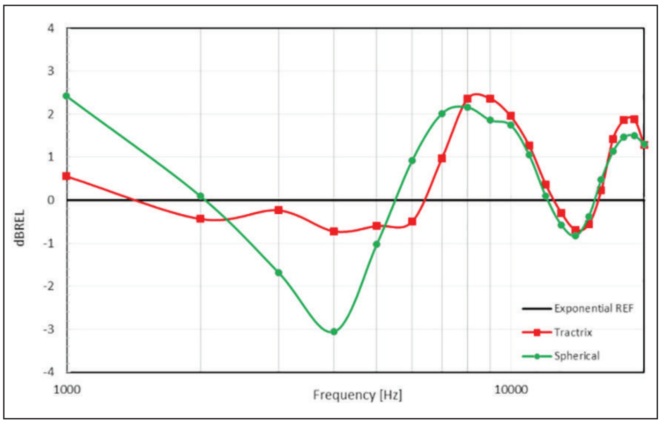

Figure 15: This is the normalized exponential horn frequency response (REF) and the relative difference of a Tractrix and a Spherical (Kugelwellen) horn referenced to the exponential one. The simulation is at 1 m distance on axis.

Minor Axis E 80.7 mm
Ratio E 1.70
Major Axis E 137.4 mm
Cursors: Cursor 1, Major Axis, X 92, Y 59
24.36 deg Alfa Major Axis from throat
30.68 deg Alfa Major Axis
100.78 mm Distance from throat Major Axis
2.18 mm Distance Major Axis
Total Points Number 61k
Fc 524 Hz
Throat Radius 17.78 mm
Flare Constant 1.0
Samples X 100
Samples Y 50
Waveguide Angle 50 deg
Temperature 25 degC
Humidity 50 %RH

Figure 18: Elliptical mouth horn's arrangement. MR = 1.7

Minor Axis E 68.0 mm
Ratio E 2.40
Major Axis E 163.1 mm
Cursors: Cursor 1, Major Axis, X 15, Y 24
22.52 deg Alfa Major Axis from throat
24.51 deg Alfa Major Axis
16.23 mm Distance from throat Major Axis
2.06 mm Distance Major Axis
Total Points Number 15k
Fc 524 Hz
Throat Radius 17.78 mm
Flare Constant 1.0
Samples X 100
Samples Y 50
Waveguide Angle 50 deg
Temperature 25 degC
Humidity 50 %RH

Figure 19: Elliptical mouth horns arrangement. MR = 2.4

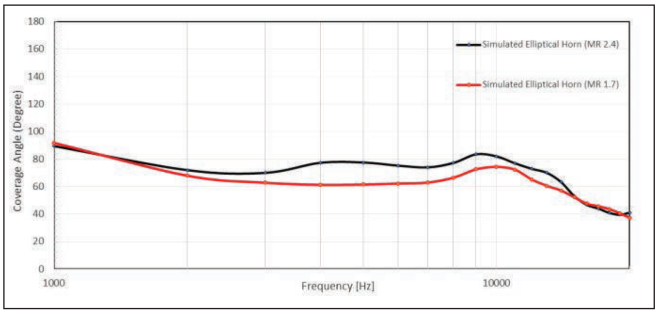

Figure 28: Elliptical mouth horn's beam-width comparison. Horn with MR = 2.4,compared to the horn with a MR = 1.7. Plane A.

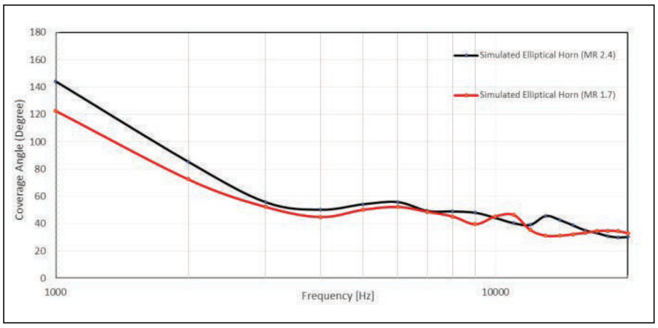

Figure 29: Elliptical mouth horn's beam-width comparison. Horn with MR = 2.4 compared to the horn with a MR = 1.7. Plane B.

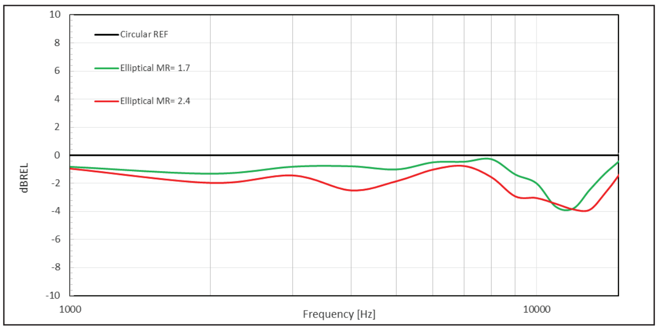

Figure 30: The normalized exponential Circular (MR = 1 REF) horn frequency response and the relative SPL difference of the same horn expansion is shown with modified mouth ratios. Elliptical MR = 1.7, Elliptical MR = 2.4 referenced to the Circular one. Simulation is shown at 1 m distance on axis.

Horn Expansion Efficiency

One of the most efficient horn expansions is the exponential profile. This horn is extraordinarily efficient as an acoustic transformer device due to its impedance match between the source of sound at the throat of the horn and the atmosphere into which the horn mouth radiates. But what is the SPL difference between a pure exponential expansion and the other types?

The horns shown in **Figure 15** were designed starting from the same values. This interesting graph shows that near the cut-off frequency the tractrix and the spherical have more pressure. This is mainly due to the natural flared mouth of these expansions, compared to the pure exponential expansion whose calculus has an unflared mouth. Then there is a range where exponential has more

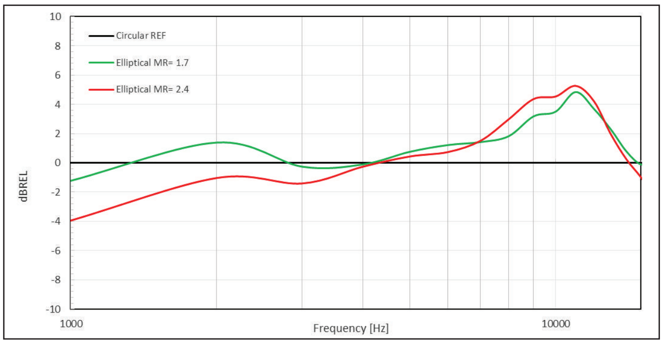

Figure 31: This is the same configuration as shown in Figure 30 but the microphone is positioned at 45° off-axis on the Plane A.

energy followed by a range where tractrix and spherical have an averaged increased SPL.

Starting from a pure exponential circular mouth profile, which produces directivity we already know for this standard horn type (see **Figure 16** and **Figure 17**), we want to obtain two different horns simply acting on the minor axis value to increase mouth ratio, defining two horns with two different ratios, MR = 1.7, MR = 2.4 (see **Figure 18** and **Figure 19**).

When MR > 1, it is not possible to build a horn only from the two axes shown in Figure 18 and Figure 19; it is necessary to use a 3D file with all 3D points in the space. In **Figures 20–27**, the directivity plots of the two designed horns are reported. Horns are in a pure exponential expansion with two different mouth ratios. The directivity of the same horns is also shown with a flare added to the original design, from which it is possible to understand the importance of a flared expansion at the horn mouth. We can read more about this point in the next section of this article.

In **Figure 28** and **Figure 29**, we can compare beamwidth of the two elliptical horns. The two mouth ratios have a different constant coverage angle on the Plane A, useful for a different application, respectively 65° (MR = 1.7) and 75° (MR = 2.4). Furthermore, when increasing MR, we are also increasing the constant directivity.

Analyzing the sound pressure between the circular horn and the elliptical one, we can see in **Figure 30** the relative SPL difference. Obviously, the circular horn has more energy because its beam width is focused on axis, while elliptical one have a spread energy around the space because they cover a bigger angle on the Plane A. Due to its structure, the elliptical horns cover a larger area and for this reason, we have an SPL loss. Instead, it's interesting to see that the decibel loss for the two elliptical horns is not too much compared to the circular one. Moreover, a decibel loss is controlled for a great portion of the frequency band.

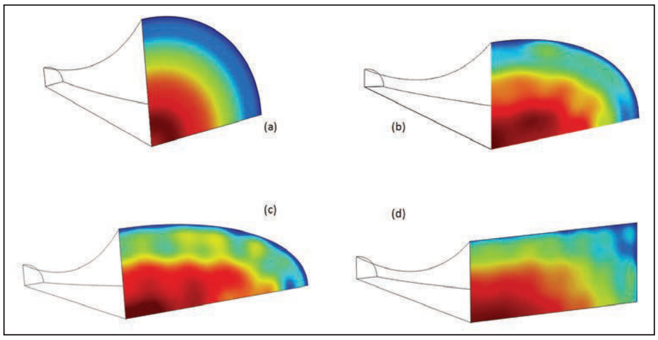

Figure 32: Horn mouth sound pressure distribution at 10 kHz. Circular (a), Elliptical MR = 1.7 (b), Elliptical MR = 2.4 (c), Rectangular MR = 2.4 (d)

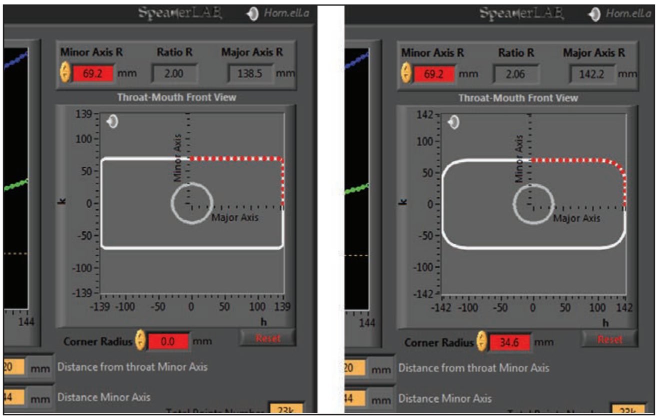

Minor Axis R 69.2 mm Ratio R 2.00 Major Axis R 138.5 mm

Corner Radius 0.0 mm

Minor Axis R 69.2 mm Ratio R 2.06 Major Axis R 142.2 mm

Corner Radius 34.6 mm

Figure 33: This is the corner radius adjustment for square and rectangular mouths. Radius = 0 and radius > 0.

Also, we can see that when increasing the MR value we increase a decibel loss on-axis, because of an SPL off-axis on Plane A intensification. Indeed, when simply moving the microphone 45° off-axis, we can see in **Figure 31** an interesting difference among the horns. For example, the elliptical MR = 1.7 has more SPL on the greater part of the frequency range compared to circular.

Today, with available simulation tools, is very simple to plot a horn mouth sound pressure distribution matrix. Next, **Figure 32** shows a one-quarter solid model of the before-mentioned horns, with the relative surface mouth SPL distribution plots for the center band frequency: 10 kHz.

As shown in Figure 32d the rectangular horn, compared to the elliptical ones, suffers of the "corner effect," which is because of reflections. For every single frequency we will have a different behavior near the corner and it can influence the wave-front distortion and the horn's general performance. About this point, elliptical mouth horns are better than rectangular ones. **Figure 34** and **Figure 35** are useful for a comparison with the other presented directivities.

In Horn.ell.a, a design section related to square and rectangular mouth horns has been added (which will be available soon) and in this section it's possible to add a corner radius (see Figure 33). To reduce wave-front

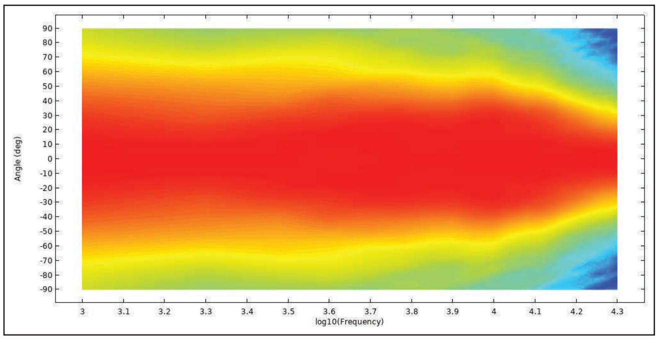

Figure 34: Rectangular flared mouth (M R= 2.4) exponential horn directivity Plane A

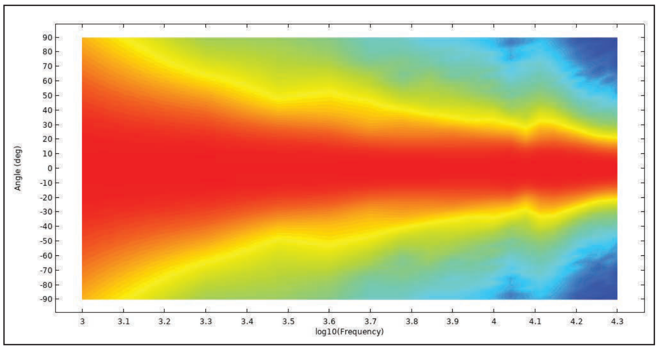

Figure 35: Rectangular flared mouth (MR = 2.4) exponential horn directivity Plane B

deformations, maintaining a constant directivity on Plane A, the software will adapt the progressive shape of the corner on each volume step, from throat to mouth.

Horn Wave-Front Shape

Analogous to the coverage angle, the coverage area is defined as the area limited by the isobar having a level of 6 dB below the maximum value found on the sphere. The coverage area gives useful information about the horn wave-front shape. The HCD horns generate a wave-front shape with a flat zone that has a contour similar to the horn mouth that generates it. In **Figures 36–38**, some examples of the wave-front shape at 10 kHz of the analyzed horn models are shown.

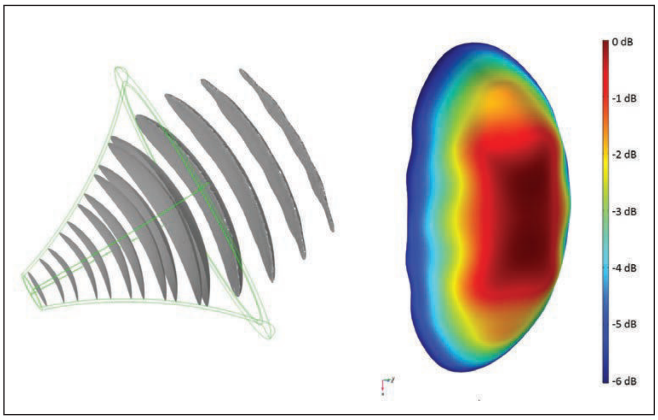

Figure 36: Wave-front shape (left) and particular of the coverage area (right) of the elliptical flared mouth (MR = 1.7) exponential horn

Mouth Diffraction Effects

There are two studies published by D. B. Keele, Jr. in the early 1970s that disclose the importance of mouth flares. The first is "Optimum Horn Mouth Size" presented at the 46th Audio Engineering Society (AES) Convention, while the second one was in Appendix 2 of the preprint 1038 presented at the 51st AES Convention. Some types of horns have a flared mouth, tractrix, and spherical horn expansions, while the hypex family horns (exponential is included in this family, flare constant T = 1) has an unflared mouth.

Now we'll see the differences in the directivity polar patterns between a standard exponential horn compared to the same shape but with a flared mouth. From the graph

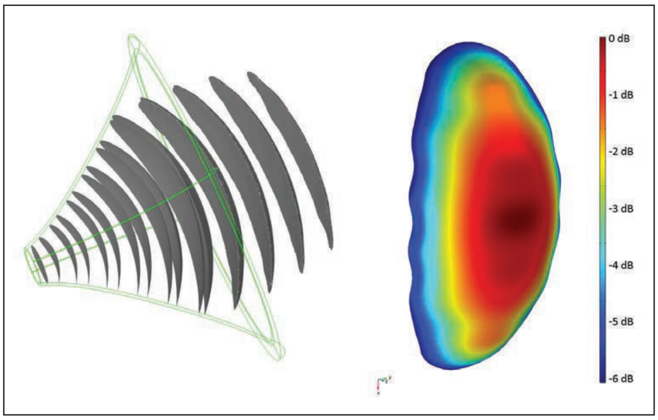

Figure 37: Wave-front shape (left) and particular of the coverage area (right) of the elliptical flared mouth (MR = 2.4) exponential horn

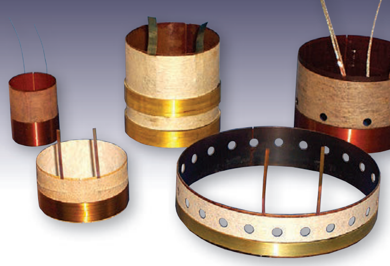

shown in **Figure 40**, we can see the frequency response deviation of the circular mouth exponential horn with a flared end loop, from Figure 39, along its mouth profile.

Figure 41 shows the same comparison but related to the elliptical mouth exponential horn (MR = 2.4), using a similar flared end as shown in Figure 39. The flare shape is not optimized for a specific application and it's shown for the higher mouth ratio (2.4) horn, because it represents the worst case.

Analyzing the elliptical mouth exponential horn (MR = 1.7) polar patterns shown in **Figure 42**, we can see that on the constant directivity Plane A, the flared mouth has a very small influence on the off-axis horn performance, because the wave-front is guided by the pseudo-conical shape. In Plane B, shown in **Figure 43**, the flared mouth has a significant influence due to acoustic pressure diffractions, as the wave-front expands with the exponential progression.

As I mentioned earlier, there is not a unique profile to build a flared mouth, but we need to differentiate it along the loop. Resuming, with the horn constant directivity profile, Plane A, we can reduce the flare dimension as it has a minor impact. On the contrary in Plane B it has a great importance and it must be accounted for to obtain a good directivity, frequency, and impulse response at the same time. The frequencies where we can find problems on directivity polar patterns depend on the horn's geometry, dimension, and expansion and in this case are in the range 5÷8 kHz.

Please note that the according to a polar pattern analysis for a horn application in full space (4π steradian solid angle), indeed the problems could be outside the

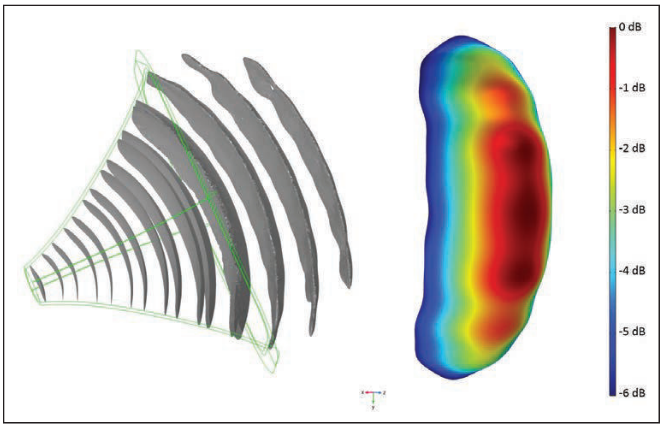

Figure 38: Wave-front shape (left) and particular of the coverage area (right) of the rectangular flared mouth (MR = 2.4) exponential horn

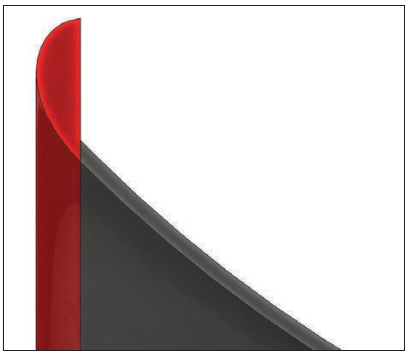

Figure 39: Here is an example of the simple flared end (solid part in red) added to the exponential expansions horn mouth profile.

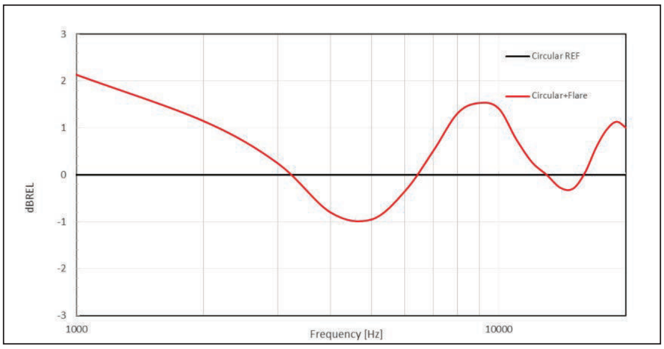

Figure 40: Normalized on-axis frequency response curve of the circular mouth exponential horn with the flared mouth (red), referenced to the same horn with the unflared mouth (black)

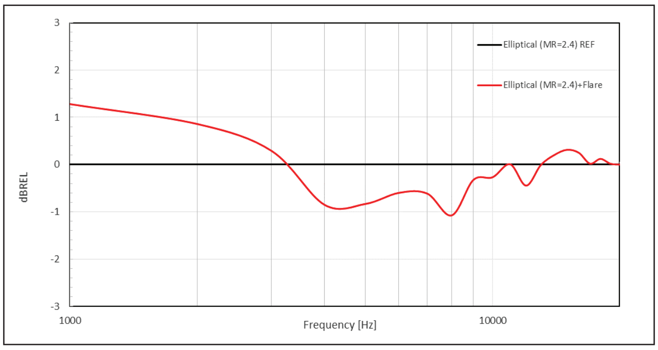

Figure 41: Normalized on-axis frequency response curve of the elliptical mouth exponential horn (MR = 2.4) with the flared mouth (red), referenced to the same horn with the unflared mouth (black)

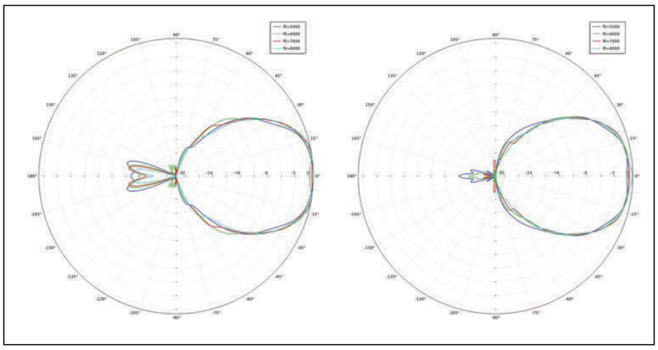

Figure 42: Elliptical mouth exponential horn (MR = 1.7) polar patterns on Plane A. Unflared (left) and flared mouth (right)

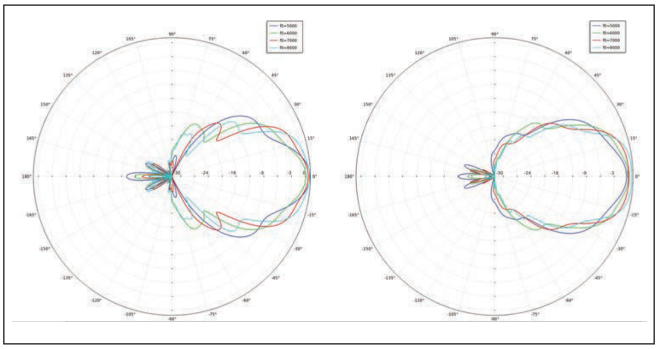

Figure 43: Elliptical mouth exponential horn (MR = 1.7) polar patterns on Plane B. Unflared (left) and flared mouth (right)

horn coverage angle, but when we apply the horn in half space (2π steradian), meaning that horn is applied on a panel, the flared mouth could have a different result. Underlining that the flared mouth shown in Figure 39 is not designed for a 4π steradian application, but it is specific for 2π steradian.

In general for 2π steradian it is also necessary to study the interactions between the horn mouth and other obstacles influencing directivity, frequency, or impulse response (e.g., if the horn or the other loudspeakers are flush mounted.

Conclusion

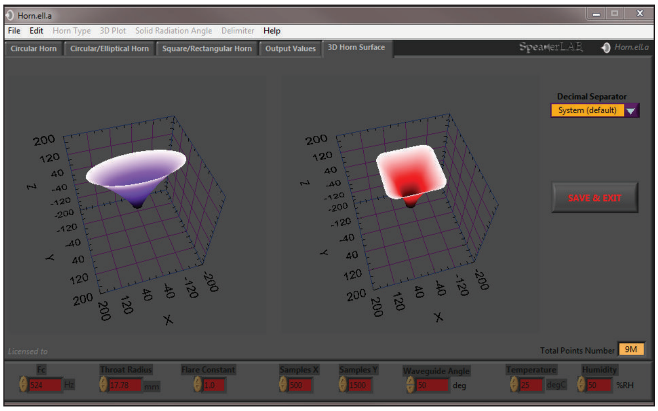

Decimal Separator: System (default)
Total Points Number: 9M
Fc: 524 Hz
Throat Radius: 17.78 mm
Flare Constant: 1.0
Samples X: 500
Samples Y: 1500
Waveguide Angle: 50 deg
Temperature: 25 degC
Humidity: 50 %RH

Figure 44: Horn.ell.a 3D horn surface reconstruction example

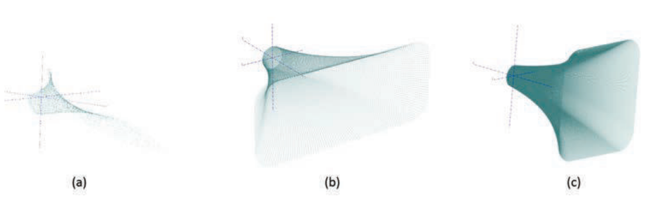

Figure 45: CAD model when open shows a .asc file. Quarter model (a), full angle model (b), model with a finer resolution (c).

In this article I have presented a new type of horn, investigating some practical aspects of constant directivity horns design through real and FEA simulated prototypes. I called the new horn family Hybrid Constant Directivity (HCD) horns. All horns described here have been designed with SpeakerLAB Horn.ell.a 2.0, without any CAD modification on acoustic boundaries. The only particulars designed externally by Horn.ell.a are the mouth flare adapters for exponential horns. For mouth ratios greater than 1, Horn.ell.a calculates HCD horns regardless of the selected expansion.

The latest Horn.ell.a version, shown in **Figure 44**, manages circular/elliptical and square/rectangular horns at the same time, saving them directly in a 3D file extension .asc. This is a standard code for information exchange ASCII encoding file, easy manageable by most CAD systems available today. When opening the .asc file with your CAD, you can see the model as shown in the **Figure 45**. More information about SpeakerLAB Horn.ell.a is available at www.speakerlab.it.

Last, I would like to thank Alfred Svobodnik and Giovanni Di Gesù for technical examination and proofreading. ***VC***

Focus: MEMS Loudspeakers

The Coming Impact of MEMS Audio in 2020

By Mike Klasco (Menlo Scientific, Ltd.)

The consumer electronics industry at-large has been able to digitize and shrink most of the device components and electronics. One of the last remaining barriers is the speaker—it remains comparatively heavy, bulky, and restrictive. This month, we explore new technology microspeakers and their challenges to transform the consumer electronics industry as microelectromechanical systems (MEMS) did to electret condenser microphones (ECMs). MEMS is the technology of very small devices, usually consisting of a micro-sensor/transducer and an application-specific integrated circuit (ASIC) that processes data or in the case of MEMS speakers amplification and codec functions.

Back in January 2015, I gave a talk on MEMS loudspeakers at the Association of Loudspeaker Manufacturing & Acoustics (ALMA) International's Symposium and Expo (AISE) and followed that discussion with an article in the pages of *Voice Coil*. Five years later, and the time is now ripe for an update survey of MEMS audio technology—what is just now reaching the market and what is coming. This month's focus centers on microspeakers and earphones, with MEMS microphones coming up next.

We will examine MEMS devices in general, provide a basic explanation of how the various types of MEMS speakers work, and what commercialization challenges are ahead. As the first MEMS speakers are now becoming viable commercial products, we also need to consider their practical applications, unit costs, and acoustical strengths and weaknesses.

So now it is reality check time—Could MEMS loudspeakers signal the end of speakers as we know them? As MEMS speakers are just starting to evolve into viable commercial products, what might be the impact on the speaker industry, practical applications, projected unit costs, and acoustical strengths and weaknesses? For decades, MEMS microphones were all show and no go. Yet progressively over the last few years, they have come to dominate the mobile audio device market. On the other hand, ATCO's hypersonic array speaker was also supposed to take over the industry—but that was more of a stock market exercise—and today, it is only a boutique application. NXT's distributed mode loudspeakers (DML) also supposedly signaled the "end of the world for existing speaker technology," but even 20 years later this flat-panel topology's current proponents are still fighting for market share. The Tymphany linear array transducers (LATs) of a decade ago showed another different path to sound reproduction. Currently, Tymphany is successfully producing conventional but well-executed speaker designs and no longer offers LATs.

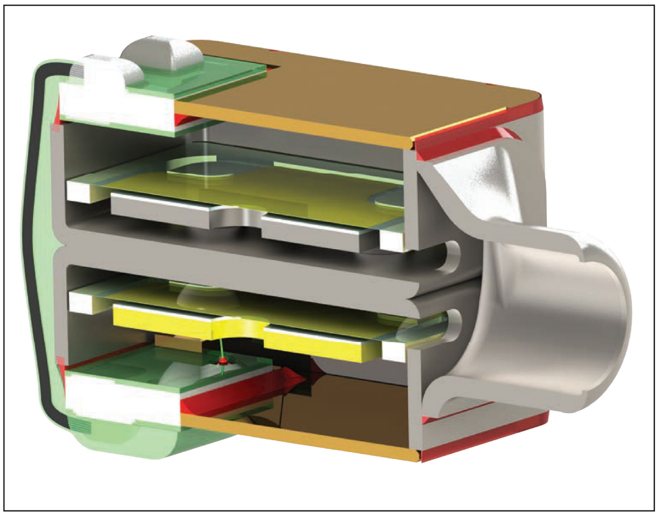

This is a crosssection of an electrostatic IEM tweeter developed by Sonion, which designs and manufactures cutting-edge audio components and provides complete solutions to its customers who then manufacture hearing aids, in-ear earphones and hearables/wearables.

With these past "not-quite game changers" still fresh in our memories, how might MEMS speakers fit into the speaker industry? It is clear that speakers are going to be a tough application for MEMS technology as speakers need piston area and excursion to move air. The verdict is MEMS speakers might take some time to come to fruition.

A Bit of MEMS History

MEMS development over the last three decades has been slow and painful. The semiconductor industry's favorite joke regarding MEMS development roadmaps are that they are calculated in dog years (seven times that of human years). However, MEMS devices became practical when they could be manufactured with high yields using integrated circuit (IC) fabrication and device packaging processes.

MEMS devices include microphones, accelerometers, vibration/shock sensors (e.g., burglar alarms and airbag sensors), gyros and now microspeakers and earphone transducers. The implementation of MEMS speakers is daunting compared to mics due to the far higher excursion requirements. Yet even the promise of MEMS microphones was slow to be achieved, with many development teams in the 1990s eventually giving up. Venture capital investments in MEMS mic startups rarely reached successful outcomes as the investors just did not have the staying power to keep pouring funds into research and process control.

There are quite a few steps in MEMS fabrication and getting high yields on every step always seemed to be another development phase away. It took more than 20 years for the first billion MEMS microphones, and two years for the second billion's production, compared with monthly production now reaching about 1 billion monthly. Today, MEMS microphones totally dominate smartphones, tablets, laptops, portable media players, speech recognition systems, personal computers, surveillance cameras, 3D cameras, radars, anti-theft alarms, headphones, smart speakers, music recorders, and various smart home voice command

appliances, including air conditioners, refrigerators, and service robots.

Back to the MEMS Microspeaker

The microspeaker and earphone driver market is about $10 billion annually. Just considering the work needed to shift production lines, even automated speaker production line manufacturing, over to semiconductor foundries is mind boggling. The titans of microspeaker manufacturing typically have about 50,000 employees, while MEMS foundries producing similar quantities of devices have staffs of less than 500. Yes, the wafers from the foundry will still need to be "packaged" but a few zeros in workforce numbers are still lobed off…) With the rising cost of salaries in China, MEMS microspeakers will have a dramatic impact on staffing along with other far-reaching implications. But it is not just the fabrication of the transducers, but the promise of automated pick-and-place of MEMS speakers for surface-mount technology (SMT) board stuffing rather than hand soldering of billions of speakers. Let's ponder practical applications, projected unit costs, and acoustical strengths and weaknesses.

While MEMS microphones have taken the lion's share of the microphone market, why are the microspeaker transducers almost 100% electro-dynamic (magnetic structure with a voice coil)? The 800 lb. gorilla blocking MEMS speakers is "pumping power." While the micro-mechanism in MEMS mics only need to have enough movement to respond to the acoustic signal, MEMS speakers need to move air. But even MEMS mics have so little excursion capability that the acoustic overload point (AOP) is a serious consideration in spec'ing MEMS mics.

Some MEMS mics will latch up (the diaphragm will stick to the plates) if what they are mounted into is dropped or even if a car door is slammed. With conventional speakers, acoustic physics for sound output is the Xmax (excursion) times the piston area. The typical smartphone speaker diaphragm footprint is 10 mm × 15 mm and has about 0.5 mm Xmax peak excursion. The air moving power of MEMS speakers is significantly less than even the lowest performance microspeakers.

In every case of the unique transducers surveyed here, output is minuscule and outside of the application to in-ear monitors (IEMs) or hearing aids, they must be used in multiples. USound describes MEMS speakers as the "LED of the acoustics," and the size and configuration of the array would be application-specific. Multiple speakers means multiple cost. Many of transducers here are made from wafers, which are sliced and diced and then packaged into complete speakers, much like MEMS mics. Wafer costs could be $500 to more than $1,000 depending on the process and diameter of the wafer. Using advanced math, if you need two (or four or half a dozen) MEMS devices for your application, the costs of both the the wafer and the packaging starts to add up quickly.

Speaker engineers following conventional wisdom means that for achieving the required sound levels and bass response, you need to have a large enough diaphragm moving far enough. Some of the new contenders point out their sound production technology does not follow the conventional physics of moving diaphragm transducers. Just a caveat here, perhaps the rules are different but they may come with a new set of problems.

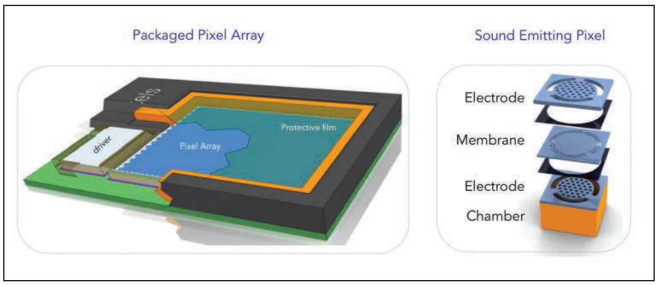

Audio Pixels is one of the pioneers in the development and production of MEMS digital speaker chip technology. Its silicon chip can be used either as a stand-alone speaker or cascaded in any multiples of the same chip to achieve required performance specifications.

The "Holy Grail" for these alternative MEMS speaker technologies is to become the next smartphone microspeaker. There are more than 1.6 billion mobile phones produced each year, each with at least two microspeakers—a receiver and speakerphone transducer. Less "pumping power"is required for headphones than speakerphone applications, still less for earphones (and hearing aids) and even less for earphone "tweeters."

MEMS speakers promise to be ideal receivers for in-canal hearing aids and implantable hearing devices (i.e., cochlear and auditory brainstem implants). These applications have very small "air pumping volume" required for adequate acoustic output due to the enclosed duct and close proximity to the middle ear. A more ambitious step are in-canal IEM earphones, which require not much more acoustic output than implantable transducers. Between these two applications, IEM tweeter transducers are another application (many IEM earphones are two-way or more designs using balanced armature drivers).

The first MEMS speakers have already reached the market. There are a handful of MEMS solutions that replace conventional voice coil actuator with MEMS mechanisms while others are not precisely MEMS, but all are relevant for earphone and microspeaker applications. Each of these designs has significant development and manufacturing barriers to mass acceptance and productization.

Piezo Speakers

One of the promising technologies is piezo speakers which already have a long history in the speaker industry. Motorola's ceramic horn tweeters were used in pro-sumer speakers by the millions for decades. Piezo microspeakers have very low profiles, which are highly desirable for smartphones, and there has been a half dozen short-lived piezo microspeakers. The challenge has always been the limited excursion along with lack of adequate bottom-end or even lower midrange output. The redeeming aspect of piezo transducers is that while excursion of the ceramic element is limited, this can be somewhat addressed with larger and thinner ceramics, but also as the force of the ceramic element is high, enabling a cantilever to increase excursion.

Now for our survey of these next-generation devices including an overview of their technology and development status. Additionally, we have provided a directory of this eclectic group of diverse technologies (see page 24).

USound

USound is a fabless audio semiconductor company offering piezo silicon speakers based on MEMS technology. USound was able to overcome the limitation of traditional piezo transducers, and with its innovative MEMS concept have proven that they can generate relatively large displacements. USound has developed and shipped several hundred thousand of what it believes are the smallest and first MEMS loudspeakers in the world.

USound's Andrea Rusconi pointed out that their major selling points, confirmed by customers, are form factor and weight along with reflow solder compatibility. Reflow soldering was the one major motivation for the breakthrough of MEMS microphones in consumer electronics. USound's solution with its MEMS processes (including microelectronics-grade packaging) works better for speaker manufacturing but also at product level because reflow soldering of the speaker enables audio modules manufactured in SMD lines with integrated electronics (i.e., connectivity, sensors etc.). Another major advantage of USound's MEMS loudspeakers is their flexibility, with different versions for in-ear and also speaker applications. USound microspeakers are currently offered for smartphones, earbuds, audio modules for augmented reality and virtual reality glasses, and numerous consumer wearables, as well as 3D surround sound headphones. Together with production partners STMicroelectronics, Flex and AT&S, USound has implemented a global semiconductor supply chain.

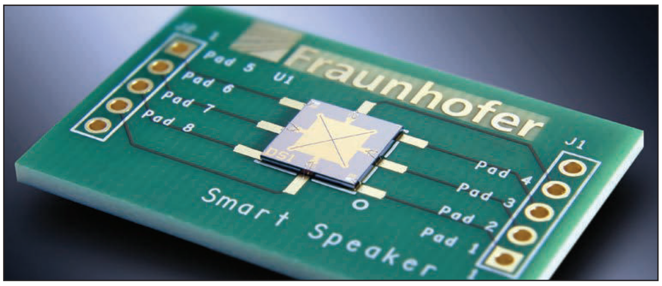

Fraunhofer, the German research institute is developing both piezo and capacitive (electrostatic) all-silicon MEMS-speakers. Its CMOS-compatible MEMS speaker is based on electrostatic bending actuators.

TDK

TDK, best known for its sensors and electronics components, based its PiezoListen microspeakers on a haptic device. Twelve layers of piezoelectric material are stacked so that displacement and maximum sound level is increased with response down to 200 Hz. Intended for

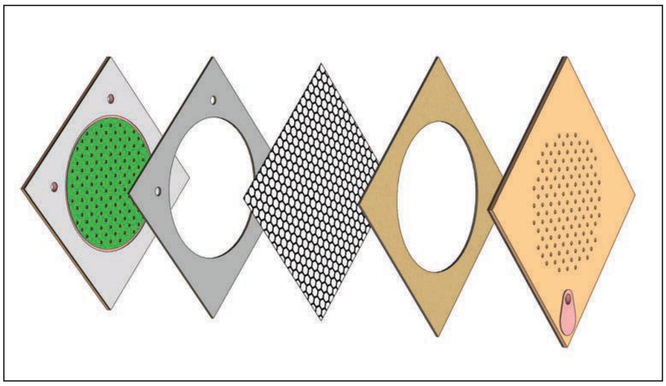

GraphAudio has developed an electrostatic driver where the pure graphene diaphragm functions as part of the "motor." Here is an exploded view of an 8 mm speaker assembly.

consumer products such as tablet computers and TVs. The speaker comes in two types: a "wide-range" type and "high-range" type. The wide-range type bandwidth is 400 Hz to 20 kHz. Though it does quite reach the low-end response of conventional speakers, it is adequate for tablets and laptops.

Ultrasonic heterodyne sound generators has had their proponents and commercial audio designs from ATCO, Holosonics (Spot Light) and others, but these have been shoebox to ceiling tile size implementations. Work continues on MEMS implementations of ultrasonic heterodyne, ultrasonic shutter modulation, and digital sound reconstruction for microspeakers. Questions remain on achieving signal reproduction integrity, issues with the high levels of ultrasonics generated to achieve adequate audio levels, and attaining usable low-end frequency response.

Audio Pixels

Audio Pixels is one of the pioneers in the development and production of MEMS digital speaker chip technology. The company is directly generating sound from a digital audio stream. Audio Pixels holds innovative patents in the fields of electromechanical structures, pressure generation, acoustic wave generation, and control, signal processing, and packaging. Its silicon chip can be used either as a stand-alone speaker or cascaded in any multiples of the same chip to achieve required performance specifications. This modular paradigm is comparable to "parametric speakers" such as phased arrays or using more transducers for increasing the dynamic range.

Audio Pixels' Digital Sound Reconstruction (DSR) technique is based on a theory introduced by Bell Labs in the 1930s. Originally a secure "digital" speech vocoder for military communications with a "digital speaker" to reconstruct the speech. The sound wave is generated from the summation of discrete pulses that are produced from an array of pressure generating micro-transducers. Within each transducer is an array of identical elements fine-tuned to a particular frequency. As with analog speakers, different frequencies are produced by varying the timing of the motion. Proof-of-concept continues to progress. Audio Pixels is in partnership with Sony as one of its MEMS foundry partners and ICsense for the ASIC design.

GraphAudio

GraphAudio licensed the graphene audio work and patents from The Lawrence Berkeley National Labs in 2016 for development of commercialized audio products. GraphAudio has developed an electrostatic driver where the pure graphene diaphragm functions as part of the "motor." Its initial products are earphones using a graphene diaphragm sandwiched between electrodes. When this field oscillates due to the audio signal, it causes the graphene to vibrate in a physical analogy to the audio electrical signal and this generates sound. It's essentially an electrostatic speaker; but instead of a metalized polymer film diaphragm, graphene is used. Also in development is a studio microphone and super wideband measurement mic.

Graphene diaphragms are very thin and light with a small spring constant so that the air itself damps its motion. The symmetrical push-pull electrostatic drive has been the core technology of the finest audiophile headphones and speakers and studio microphones. The ability to power graphene earphones and speakers using conventional mobile battery power expands their application from just the boutique end of the market. Batteries for the DC bias, work for graphene since they source only voltage and virtually no current. Since the power is tiny, there is no need for high current and small batteries suffice. Demonstration earphones have been produced and demonstrated with audiophile quality results.

Fraunhofer

Hedging its bets, Fraunhofer, the German research institute is developing both piezo and capacitive (electrostatic) all-silicon MEMS-speakers. Its CMOS-compatible MEMS speaker is based on electrostatic bending actuators. Future work will focus on increased SPL and reduced distortion through optimized actuator design. Concurrently, development continues on a piezoelectric MEMS with concentrically cascaded lead zirconate titanate actuators making it the first integrated two-way MEMS speaker.

Designed to operate without a closed membrane to improve the acoustic performance, energy efficiency, and manufacturability. Extensive finite element analysis studies revealed an SPL of more than 79 dB in 10 cm distance at 500 Hz for a device 1 cm^2 in size operated at 30 V. At higher frequencies larger SPL values are calculated enabling a flat frequency response with 89 dB for frequencies above 800 Hz. Based on this concept, first speaker prototypes have been fabricated.

Sonion

Sonion's electrostatic IEM tweeter (electret) is designed for a smoother, more clean sound in the higher frequencies than traditional balanced armature IEM's using standard tweeters. The Sonion electrostatic super-tweeter produces high frequencies from 7 kHz and upward. The driver comprises a specifically arranged dual electret cartridge that lowers symmetric distortion combined with a miniature transformer. This enables electrostatic performance in IEMs without the usual separate power supply for stepping up the voltage and supplying bias to the driver. The result is stunning audio quality with crystal clear undistorted sound that goes well beyond the limits of human hearing. The dimensions of their electrostatic tweeter are 3.55 mm × 3.55 mm × 2.54 mm (32 mm^3), a single version is also available and measures 3.55 mm x 3.55 mm x 1.27 mm (16 mm^3).

xMEMS Labs

xMEMS Labs, a California MEMS startup has developed a MEMS speaker initially for earphone applications. Promising transducers of small size and low power consumption, with scalable design enabling the application's SPL requirement defining the number and arrangement of "speaker cells." Specifically a handful of cells may be sufficient for earbuds, but smartphones may require more. xMEMS claims ability to reach a range of frequencies as low as 20 Hz at least half the size of a conventional dynamic microspeaker. While xMEMs has not yet revealed specifics on its MEMS speaker technology, it is developing a complete MEMS process that reduce the manufacturing complexities which integrate the membrane and actuator making it uniquely capable for high-volume MEMS manufacturing. If you are curious, check out their patent on an "Air Pulse Generating Element and Sound Producing Device."

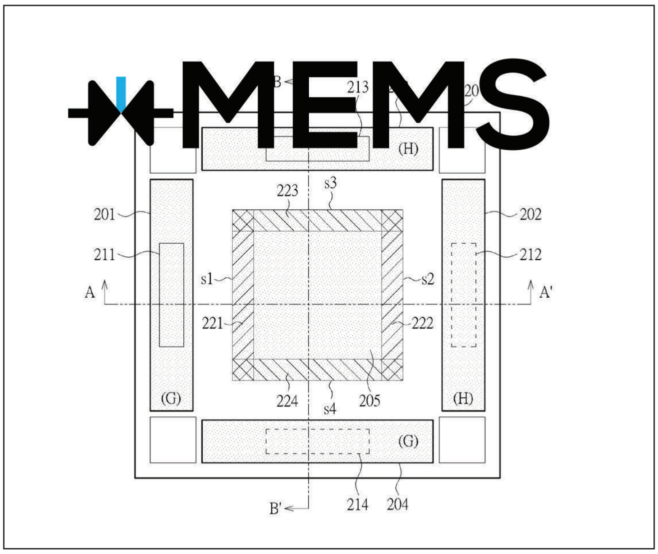

xMEMS Labs, a California MEMS startup has developed a MEMS speaker initially for earphone applications.

This MEMS speaker survey is just the tip of the iceberg as I know of other initiatives that are still in the stealth mode. But as with MEMS microphone development, many of these efforts will dead-end, at least until the technology infrastructure catches up. ***VC***

2019 MEMS Loudspeaker Directory

By Nora Wong (Menlo Scientific, Ltd.)

Audio Pixels, Ltd.
3 Pekris St., Rehovot 76702, Israel
Contact: Danny Lewin (CEO)
P: +972-(0)-73-232-4444
info@audiopixels.com | www.audiopixels.com.au

Audio Pixels is a pioneer in the development of MEMS digital speaker chip technology. Directly generating sound from a digital audio stream, its silicon chip can be used either as a standalone speaker or cascaded in any multiples of the same chip to achieve required performance specifications. Within each transducer is an array of identical elements fine-tuned to a particular frequency. As with analog speakers, different frequencies are produced by varying the timing of the motion. Proof-of-concept on the microspeaker continues to progress.

Fraunhofer Institute for Digital Media Technology IDMT
Ehrenbergstraße 31 98693 Ilmenau
Contact: Dr.-Ing. Daniel Beer (Head of Electroacoustics,
daniel.beer@idmt.fraunhofer.de)
P: +49-3677-467-385
https://www.idmt.fraunhofer.de/en.html

Fraunhofer, the German research institute is developing both piezo and capacitive (electrostatic) all-silicon MEMS speakers. Their CMOS-compatible MEMS speaker is based on electrostatic bending actuators. Future work will focus on increased SPL and reduced distortion through optimized actuator design. Concurrently, development continues on a piezoelectric MEMS with concentrically cascaded lead zirconate titanate actuators making it the first integrated two-way MEMS speaker. Based on this concept first speaker prototypes have been fabricated.

GraphAudio
Lorance Wilson (lwilson@graphaudio.com)
P: 650-260-8675
https://www.graphaudio.com

GraphAudio's electrostatic driver boosts a pure graphene diaphragm functioning as part of the "motor." Its initial product is an earphone using a graphene diaphragm sandwiched between electrodes. It's essentially an electrostatic speaker; but instead of a metalized polymer film diaphragm, graphene is used. The ability to power graphene earphones and speakers using conventional mobile battery power expands the application from just the boutique end of the market. Demonstration earphones have been produced and demonstrated with audiophile quality results.

ORA Graphene Audio, Inc.
780 Ave., Brewster RC-016, Montreal, Quebec,
H4C 2K1, Canada
Robert-Eric Gaskell, Ph.D. (Co-founder,
robert.gaskell@ora-sound.com)
P: 877-404-9033
www.ora-sound.com

ORA has developed GrapheneQ, a graphene oxide material that can be used for diaphragms and voice coil bobbins (if a bobbin is used rather than bobbinless voice coil construction). The operational range of microspeakers is directly limited by the speaker's ability to dissipate heat. Improving thermal conductivity in the former and membrane helps move heat away from the voice coil, improving the power handling. GrapheneQ is thermally conductive, helping to move heat away from the voice coil, minimizing speaker damage. A GrapheneQ speaker would also be lighter and more efficient, further increasing the speaker's output capacity.

Sonion
3655 Plymouth Blvd., Suite 103, Plymouth, MN 55446
Contact: Greg Hovland (Key Account Manager, Sales,
ggh@sonion.com)
P: 507-269-8395
www.sonion.com

Sonion's electret electrostatic in-ear monitor (IEM) tweeter provides smoother, cleaner sound at higher sound levels than the balanced armatures. Initial offering is a super-tweeter from 7 kHz. Considering Sonion's heritage with hearing aid transducers, in-ear voice is surely on the development roadmap. The electret tweeter does not have the high bias requirement of electrostatics. It is currently offered with a size of 3.55 mm × 3.55 mm × 1.27 mm.

TDK Components U.S.A., Inc.
1 TDK Blvd., Peachtree City, GA 30269-2047
P: (770) 631-0410

TDK PiezoListen microspeakers are based on a piezo haptic device. The design has 12 layers of piezoelectric material stacked so that displacement and maximum sound level is increased with response down to 200 Hz. The microspeakers are intended for consumer products (e.g., tablet computers and TVs). The speaker comes in two types: a "wide-range" type and "high- range" type. Though it does quite reach the low-end response of conventional speakers, it is adequate for tablets and laptops. Available from Mouser and other TDK distributors.

USound GmbH
Gutheil-Schoder-Gasse 8-12, 1100 Vienna, Austria

Contact: Thomas Gmeiner (VP Program Management, thomas.gmeiner@usound.com)
P: +43-676-7237499
info@usound.com | www.usound.com

USound was able to overcome the limitation of traditional piezo transducers and with its innovative MEMS concept has proven that it can generate large displacements. USound has developed and has already shipped several hundred thousand of what it believes are the smallest and first MEMS loudspeakers in the world. Key points confirmed are form factor and weight along with reflow solder compatibility.

xMEMS Labs
280 2nd St., Suite 240, Los Altos, CA 94022
Contact: Joseph Jiang (Co-founder and CEO)
P: 408-621-2996
http://xmems.com

xMEMS Labs has developed a MEMS speaker initially intended for earphone applications. The company promises transducers of small size and low power consumption, with a scalable design, enabling the application's SPL requirement defining the number and arrangement of "speaker cells." Specifically a handful of cells may be sufficient for earbuds, but smartphones may require more. xMEMS claims its product has the ability to reach a range of frequencies as low as 20 Hz at least half the size of a conventional dynamic microspeaker. While xMEMs has not yet revealed specifics about its MEMS speaker technology, it is developing a complete MEMS process that reduces the manufacturing complexities, which integrate the membrane and actuator making it uniquely capable for high-volume MEMS manufacturing. xMEMS Labs calls it an "Air Pulse Generating Element and Sound Producing Device." **VC**

Editor's Note: Voice Coil *is the only industry publication focused exclusively on loudspeakers, their design, construction, and measurement. Throughout the year we try to include a directory that coincides with our focus for each month. In 2020, our directories will include:*

- January: Headphones
- February: Cones
- April: Microspeakers
- May: Asian Components
- June: Headphones Test & Measurement
- July: Adhesives
- August: Voice Coils
- October: Digital Amps/DSP
- November: Test Microphones
- December: MEMS Loudspeakers

Sometimes companies are unintentionally omitted. If your company was not listed, please contact us. We are also working on our annual sister publication, The 2020 Loudspeaker Industry Sourcebook*. To be included, visit www.loudspeakerindustrysourcebook.com.*

Acoustic Patents

By James Croft (Croft Acoustical)

The following loudspeaker-related patent was filed primarily under the Office of Patent and Trademarks classification 181 for acoustical devices and 381 for electrical-signal processing systems and HO4R for international patents. This also includes new patent applications that are published in the *Patent Application Journal*.

Loudspeaker Enclosure with Closeable Port
Patent/Publication Number: 2019/0320257
Inventor: Jakob Dyreby (Struer, Denmark)
Assignee: Bang & Olufsen A/S (Stuer, Denmark)
Filed: December 8, 2017
Current International Class: H04R 1/28 20060101
Published/Granted: October 17, 2019
Number of Claims: 18
Number of Drawings: 13

Abstract from Patent

A loudspeaker device comprising a loudspeaker unit comprising a diaphragm with a first and second surface (such as the front and rear surface of the diaphragm, respectively) and an enclosure in which the loudspeaker unit is mounted such that the first surface of the diaphragm is in acoustic communication with the surroundings of the loudspeaker device. The device further comprises an internal cavity formed in the enclosure and being in acoustic communication with the surroundings of the loudspeaker device via an acoustic element. In the device, the second surface of the diaphragm is in acoustic communication with the internal cavity. The acoustic element can be varied between a state in which sound energy generated by the loudspeaker unit in the internal cavity can be emitted to the surroundings via the acoustic element and a state in which sound energy is substantially prevented from entering the surroundings via the acoustic element.

Independent Claims

1. A loudspeaker device comprising: a loudspeaker unit comprising a diaphragm with a first and second surface and an enclosure in which the loudspeaker unit is mounted such that the first surface of the diaphragm is in acoustic communication with the surroundings of the loudspeaker device; an internal cavity formed in the enclosure and being in acoustic communication with the surroundings of the loudspeaker device via an acoustic element; wherein the second surface of the diaphragm is in acoustic communication with the internal cavity; wherein the acoustic element can be varied between a state in which sound energy generated by the loudspeaker unit in the internal cavity can be emitted to the surroundings via the acoustic element and a state in which sound energy is substantially prevented from entering the surroundings via the acoustic element; wherein the loudspeaker device is provided with digital signal processing (DSP) filter means that interacts with the opening/closing of the acoustic element, whereby different filter adjustments can be applied to the input signal to the loudspeaker device dependent on whether the acoustic element is in an open or closed state.

15. A method for improving the sound quality especially at low frequencies of a loudspeaker device, which method comprises: providing a loudspeaker device comprising a loudspeaker unit having a diaphragm with a first surface and a second surface, wherein the loudspeaker unit is mounted in an enclosure having an internal cavity such that the first surface of the diaphragm radiates sound energy into the surroundings of the enclosure and the second surface of the diaphragm radiates sound energy into the interior cavity of the enclosure, and wherein the interior cavity is acoustically connected to an opening in the enclosure such that sound energy can enter the surroundings of the enclosure through the opening, wherein the acoustic connection takes place through an acoustic element in which the acoustic element is configured such that the acoustic element can block or open the acoustic connection from the internal cavity to the surroundings; providing activating means configured to block or open said acoustic connection from the internal cavity to the surroundings; setting a threshold value that defines whether the activating means shall block or open the acoustic connection from the internal cavity to the surroundings; providing means for determining if said threshold value is exceeded; if the threshold value is not exceeded, place the acoustic connection in the blocked state; if the threshold value is exceeded, place the acoustic connection in the open state.

Reviewer Comments

For many decades there has been an ongoing debate as to whether the acoustic suspension or vented loudspeaker is the superior enclosure type. Referring to **Figure 1**, it can be seen that from a large signal standpoint the vented

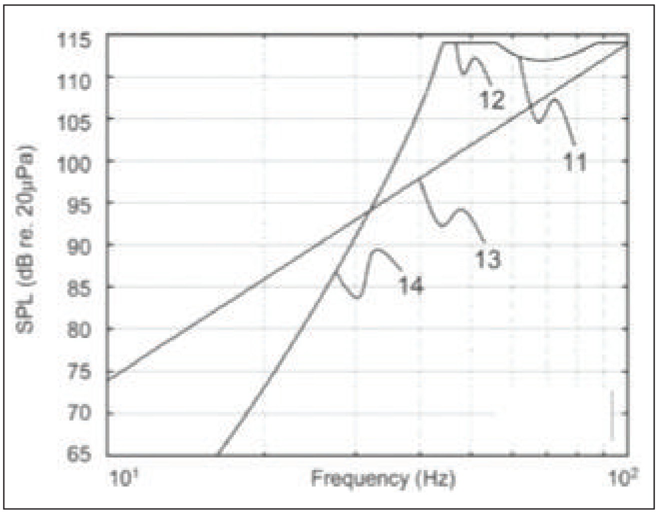

Figure 1: Large signal comparison of vented and acoustic suspension enclosure systems

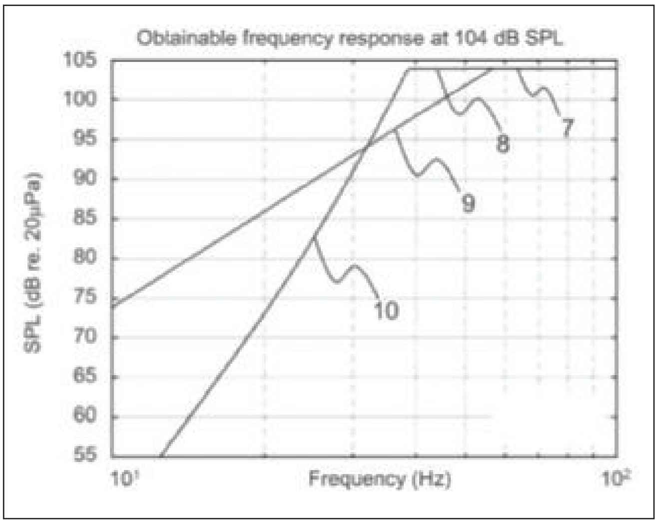

Figure 2: Small signal bandwidth comparison between vented and acoustic suspension enclosure systems

system has greater maximum linear output capability from approximately two times the tuning frequency (F_B) down to about 0.82 F_B. Whereas, the acoustic suspension system has greater maximum linear output, from approximately 0.82 F_B, down to DC. Acoustic suspension systems are preferred by many people due to exhibiting a reduced high-pass slope below cut-off, along with the associated reduction in group delay.

In the early 1970s, a number of engineers started exploring ways to integrate the two enclosure types into a combined Bass Reflex/Acoustic Suspension Hybrid, in an attempt to create a new system type that embodied the best-of-both-worlds. **Figure 2** illustrates the small signal amplitude vs frequency comparison where an ideal hybrid would maintain the uppermost curve as the system transitioned from the vented (curve 8) to acoustic suspension system (curve 9) with descending frequency.

One of the first people to examine this type of hybrid system was George Augspurger, of Perception Inc., in his 1974 Acoustical Society of America paper titled; "Dissimilar Woofers in a Common Enclosure" where he differentiated the parameters of two woofer drivers within a singular enclosure volume to create "an interesting class of quasi-ported loudspeaker systems in which one of two woofers acts as a hybrid between a loudspeaker and a passive radiator." With this basic approach, the outcome was not so much a "best of both worlds" result, but instead a continuous range of systems that fall between a sealed and vented alignment, that trades off the advantages of one for the other to varying degrees. Augspurger concluded that none of the alignments were compelling replacements for an optimized vented or acoustic suspension enclosure.

In 1975, ex-McIntosh power amplifier engineer, Mioljub "Mila" Nestorovic developed a more sophisticated version of dual-woofer, bass reflex/acoustic suspension hybrid, (See US Patent 3,984,635, "Low Range Loudspeaker System") with two woofers operated in parallel, as an acoustic suspension system, down to just above the system resonant frequency, wherein the first woofer is connected directly to the power amplifier (optionally through a crossover network) and the second woofer is connected to the amplifier through a network of a resistor in parallel with a capacitor which is attached in series with second woofer, forming a high pass shelving filter, attenuating the second woofer down in level, such that at lower frequencies, it operates as a quasi-passive radiator. This second, quasi-passive radiator woofer is adapted to have greater moving mass than the first woofer, to set a bass reflex tuning frequency (F_B). Below F_B, the shelving filter maintained just enough drive level to the second woofer to have it remain in-phase and/or remain essentially motionless, effectively sealing the enclosure so the first woofer can operate as an acoustic suspension woofer system for all frequencies below F_B, keeping the first, primary woofer from becoming "unloaded" as it would in a conventional bass reflex system, and allowing it to maintain the advantageous amplitude response of a sealed system at all lower frequencies.

The Nestorovic woofer systems were impressive performers, but also rather expensive to produce, with the second woofer requiring very large magnetics to maintain the desired QE with a long voice coil overhang to maintain linear control, while delivering the extended "passive radiator" excursions at F_B along with the series capacitor also being rather large to accommodate cut-off frequencies below 30 Hz.

The system also had two limitations that kept it from providing the ideal hybrid of a vented and acoustic suspension system. First, the reduced (but non-zero) drive to the second woofer damped the output of the "passive radiator" mode compared to a true passive radiator, or vent, keeping the system from the achieving the full "enhancement" of the Helmholtz resonance of the enclosure. The second limitation occurs because the two 8 Ω woofers are in parallel above F_B and one woofer was reduced in level at and below F_B. With a high impedance network, the system impedance transitioned from 4 Ω to approximately 8 Ω for frequencies at and below F_B, making for a less favorable impedance match to the power amplifier and sacrificing 3 dB of system sensitivity at and below F_B. That said, the system still provided the advantage of avoiding excessive excursion below F_B.

In 1978 Robert Fulton, of Fulton Musical Industries, upgraded the low-frequency section of his Fulton J-Modular

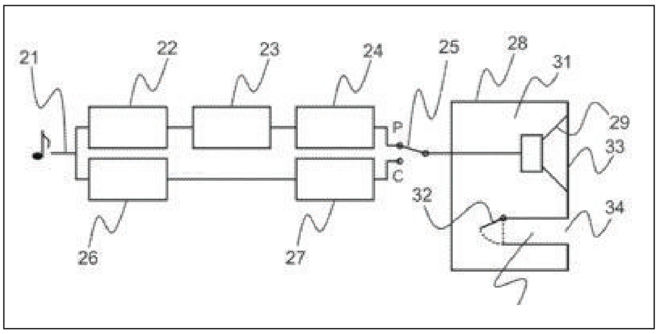

Figure 3: A schematic drawing of US Patent 2019/0320257

by adding a second 12” woofer with a very small magnet resulting in one of the configurations of the Augspurger range of dual woofer hybrid alignments, which provided a significant enhancement over the single 12” woofer acoustic suspension system it replaced.

Also in 1978, while I was working with David Graebener (then of Speakerlab, later of Bohlender-Graebener and Wisdom Audio), we developed a system that could equal the performance of the Nestorovic system while reducing cost and complexity, by re-optimizing the first woofer parameters while using a second woofer with a high impedance voice coil so that it could operate as a quasi-passive radiator while having just enough drive level to “hold still” and effectively seal the enclosure below F_B. Speakerlab produced this system for a number of years as the “Delta-i Hybrid.” This system provided a better impedance match to the amplifier, but still did not realize the full potential output at F_B due to a non-zero drive to the quasi-passive radiator.

In 1985, to satisfy our curiosity as to whether a true hybrid system could be realized that could result in a best-of-both-worlds system, we developed an advanced version that was not practical from a cost standpoint, but did realize the ideal of a bass reflex/acoustic suspension hybrid. This was achieved by applying a parallel notch filter in series with the second woofer at F_B. By doing so, were able to effectively “disconnect” the drive to the second woofer at F_B and allow it to perform as a true passive radiator at F_B while operating as a dual woofer acoustic suspension, with both woofers in parallel, above and below F_B.

To address the second issue of impedance match to the amplifier, the first woofer had two voice coils and additional series notch filter and parallel notch filters were added to maintain a substantially constant 4 Ω load throughout the low-frequency range of the system. By the time one optimized the woofers with the required maximum realizable BL and applied at least three low frequency notch filters (one version required at least five with values on the order of over 50 mH and 5,000 µF) the price of the system was increased to the extent it would be much more

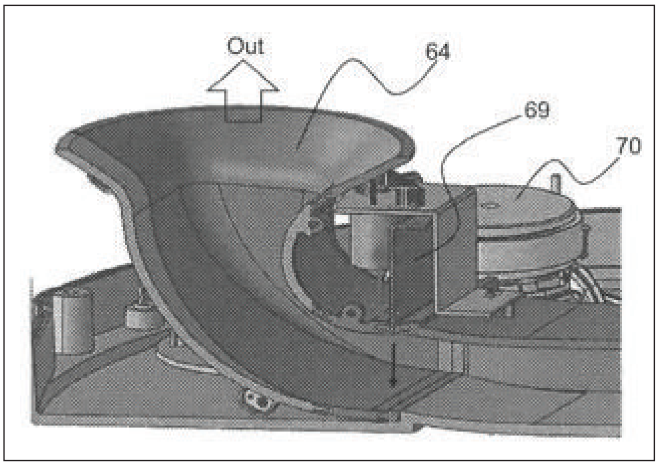

Figure 4: One of the embodiments of this invention with a linear port shutter

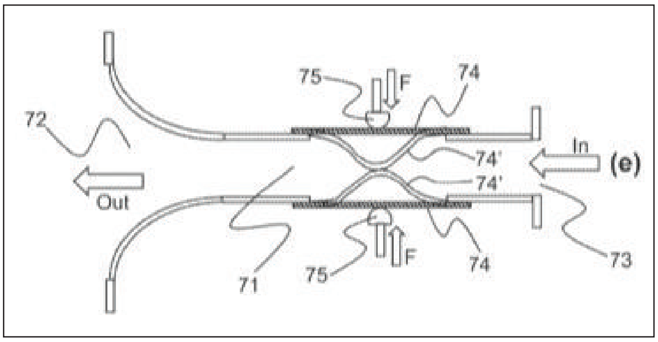

Figure 5: An embodiment of this invention with a flexible tube

cost effective to simply include a high powered amplifier and create an active woofer system. But, the exercise did verify the possibility of physically realizing the full theoretical potential of a dual-woofer system that operated as a true bass reflex/acoustic suspension hybrid.

The invention of this review recognizes the amplitude vs. frequency differences between a bass reflex and an acoustic suspension system and discloses an electro-mechanically variable port approach to realizing each system type depending on the nature of the input signal. **Figure 3** shows a schematic diagram, illustrating signal processing blocks used to adapt the state of the enclosure to be either closed or ported.

The most basic form of the system is one that is switchable between the "closed" acoustic suspension system, and the "ported" bass reflex system based on signal level and/or volume control setting. At lower signal amplitudes, the system operates as an acoustic suspension system, with more extended low-frequency capability and at high levels the system changes over to an "open port" bass reflex system with an active high-pass filter, which may simply protect the loudspeaker below tuning or act as an under-damped high-pass filter to provide a step-down bass reflex tuning providing both bass extension and low-frequency protection.

There are a wide range of embodiments that start with the basic, semi-manual, mode switching by the user or by setting of the volume control and program sensing. Other versions appear to mimic some of the variable port mass systems we have covered in these pages (e.g., US Patent 9,615,163 "Smart Bass Reflex Loudspeaker" by Ramez Nachman and Mohammed Aftab Alam, assigned to Amazon Technologies, Inc. as reviewed in the June 2018 issue of *Voice Coil*). That system disclosed tuning the port frequency by changing one or more physical properties of the port, for example by varying the length of the port, manipulating a shutter to varying degrees of openness, and varying the cross-sectional area of the port.

The current invention includes real-time versions wherein the port may be varied in cross-section or length to adapt the bass reflex form of operation before closing off the port to convert the system to a sealed, acoustic suspension

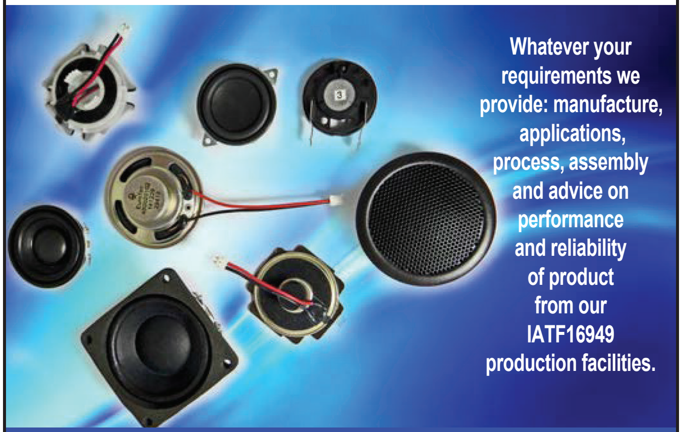

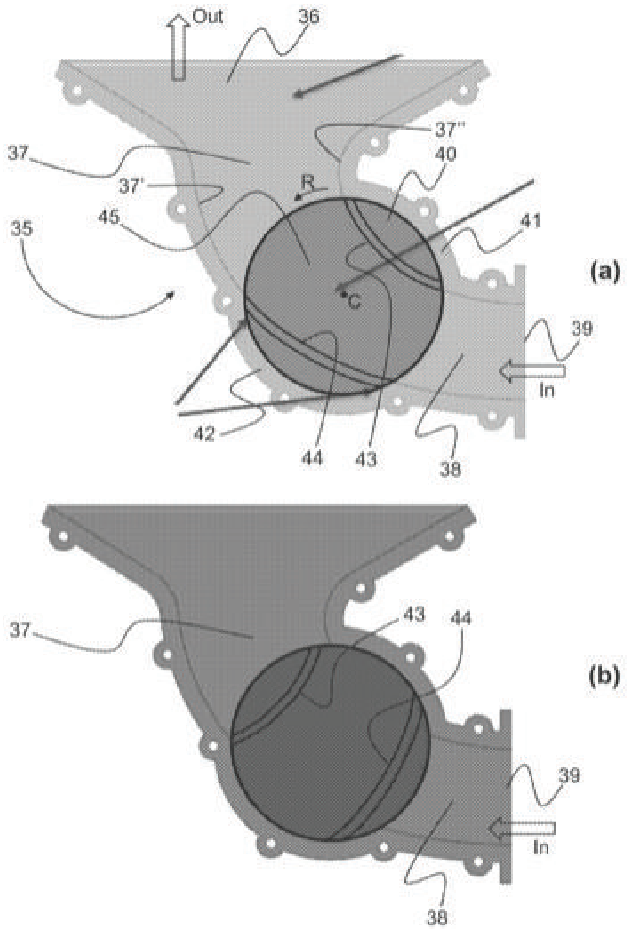

Figure 6: An embodiment of the current invention with a rotational port shutter

system. One of the mechanical port structures is shown in **Figure 4** where shutter 69 can open or close to varying degrees and transition speeds.

Figure 5 shows a variation where part of the port is constructed from a flexible tube 74, which is manipulated by actuated pistons 75 to vary the constriction of the port cross section at that point from open to closed and the points in-between. This approach, as opposed to the one of Figure 4, would at least reduce turbulence during intermediate modes of constriction.

Further embodiments, incorporate a passive radiator in place of the port and utilize a means to lock the movement of the passive radiator when the acoustic suspension mode of operation is desired. There are many more embodiments with various forms of both rotational and linear shutter systems to establish the preferred port setting for open or closed operation.

As an example of the rotational variety, **Figure 6** depicts a rotatable channel within the port, in open port mode (a) and closed port mode (b). Considering the complexity of the system being disclosed, the patent is rather meager in exploring both the required aspects of control and the various outcomes and issues to be dealt with. The idea of the delayed, look-ahead processing that would be required to change the state of the system in real-time is not explored. Also, the only comment relating to port turbulence issues is, referring to Figure 3—"The port velocity limiter 23 is only present in the signal processing path in the case where the enclosure is ported and limits the air velocity in the port in order to keep port noise at a minimum."

While using this system in its most basic configuration, to be manually switchable from one mode to the other for long-term use in a given mode, should be useful and trouble-free, the more complex modes of real-time adaptive mass and dynamically varying degrees of cross-sectional constriction of this type of mechanical system, would seem potentially fraught with a variety of sonic concerns, whether it be mechanical noise, port turbulence, or dynamic distortions similar to compressors with inappropriate attack and release times.

For those interested in studying other approaches to dynamic versions of the variable port system concept, these publications would be recommended: US application 2009/0122998, "Vented Loudspeaker Box System and Its Control Method," by Stephan Willems, assigned to Philips Electronics; and European patent WO2009/118677, "Vented Loudspeaker System," by the Ronaldus Aarts, Joris Nieuwendijk, and Okke Ouweltijes, also assigned to Philips Electronics. For dynamically variable passive radiator mass control, see US application 2017/0105065 "Passive Radiator with Dynamically Adjustable Resonant Frequency" by Joseph Pinkerton of Clean Energy Systems. ***VC***

Test Bench

A Pro Sound Transducer from Dayton Audio

By Vance Dickason

In this article, we will characterize the 2″ DMA58-4, a new full-range line array/smart speaker from Dayton Audio (see **Photo 1**). The DMA58 is nearly identical to the 3″ version, the DMA80, which appeared in the November 2019 issue of *Voice Coil* magazine. This driver is also one of the transducers from Dayton Audio's new line of full-range smart speaker/array drivers, the DMA Series. DMA stands for Dual Magnet Aluminum Cone and includes five models of full-range drivers, the DMA45 1.5″, DMA58 2″, DMA70 2.5″, DMA 80 3″, DMA 90 3.5″, and DMA 105 4″—all with both 8 Ω and 4 Ω versions.

All five models have pretty much the same feature set starting with a proprietary 12-spoke injection-molded frame. This frame is very open to reduce reflections back into the cone and also has a very generous mounting flange making multiple driver arrays cosmetically attractive and compact.

The DMA58 cone assembly consists of a black anodized aluminum cone, with a 26 mm diameter convex aluminum dust cap (directly coupled to the voice coil former), and suspended with NBR and a 45 mm diameter treated cloth surround spider (damper) for compliance. "B" for the cone assembly is supplied by a neodymium slug-type motor with an additional bucking magnet to focus flux into the gap area. Driving the assembly is a 1″ aluminum vented (five 2 mm diameter vents below the spider mounting shelf and 10 more 2 mm diameter vents above it) former wound with two layers of round copper wire. Other features include a large copper cap shorting ring (Faraday Shield) that lowers distortion and extends the high-frequency SPL profile. Tinsel leads connect on one side of the cone to a pair of solderable terminals.

I commenced testing the Dayton Audio DMA58-4 using the LinearX LMS analyzer and VIBox to create both voltage and admittance (current) curves. The driver was clamped to a rigid test fixture in free-air at 0.3 V, 1 V, 3 V, and 6 V. It should also be noted that this multi-voltage parameter test procedure includes heating the voice coil between sweeps for progressively longer periods to simulate operating temperatures at that voltage level (raising the temperature to the first and second time constants).

Photo 1: The Dayton Audio DMA58 2″ full-range transducer

Next, I post-processed the eight 550-point stepped sine wave sweeps for each of the DMA58-4 samples and divided the voltage curves by the current curves (admittance) to produce the impedance curves, phase generated by the extremely accurate LMS calculation method. I imported the data, along with the accompanying voltage curves, into the LEAP 5 Enclosure Shop software. Next, I selected the complete data set, the multiple voltage impedance curves for the LTD model, and the 1 V impedance curve for the TSL model in the transducer derivation menu in LEAP 5 and created the parameters for the computer box simulations.

	TSL Model		LTD Model		Factory
	Sample 1	Sample 2	Sample 1	Sample 2	
Fs	96.7 Hz	88.8 Hz	82.9 Hz	84.7 Hz	93.5 Hz
Revc	3.61	3.61	3.61	3.61	3.60
Sd cm2	14.5	14.5	14.5	14.5	14.5
Qms	2.30	2.24	2.24	2.18	2.40
Qes	0.49	0.49	0.52	0.50	0.56
Qts	0.41	0.40	0.43	0.41	0.46
Vas	0.15 ltr	0.15 ltr	0.18 ltr	0.18 ltr	0.14 ltr
SPL 2.83 V	82.4 dB	82.4 dB	81.8 dB	82.0 dB	86.2 dB
Xmax	2.0 mm	2.0 mm	2.0 mm	2.0 mm	2.0 mm

Table 1: Comparison data for the Dayton Audio DMA58-4 2″ full-range transducer

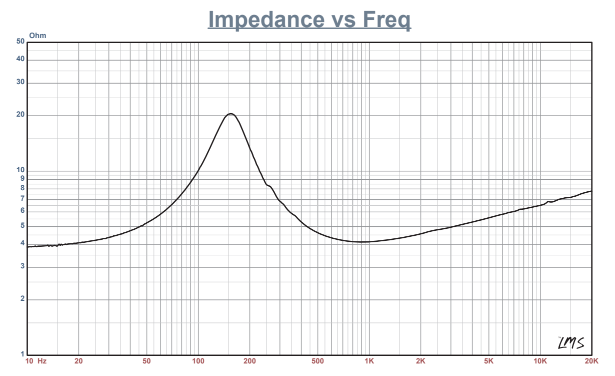

Figure 1: Dayton Audio DMA58 1 V free-air impedance plot

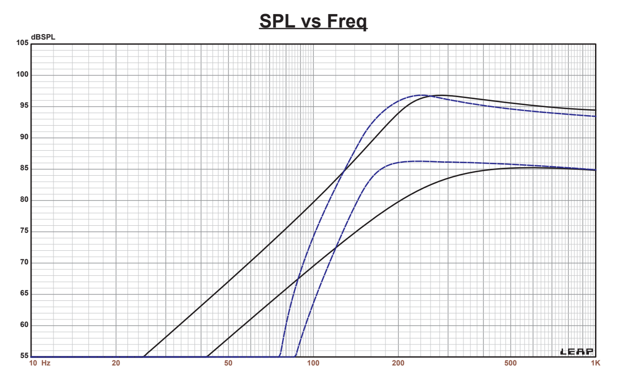

Figure 2: Dayton Audio DMA58 computer box simulations (black solid = sealed at 2.83 V; blue dash = vented at 2.83 V; black solid = sealed at 9 V; blue dash = vented at 9 V)

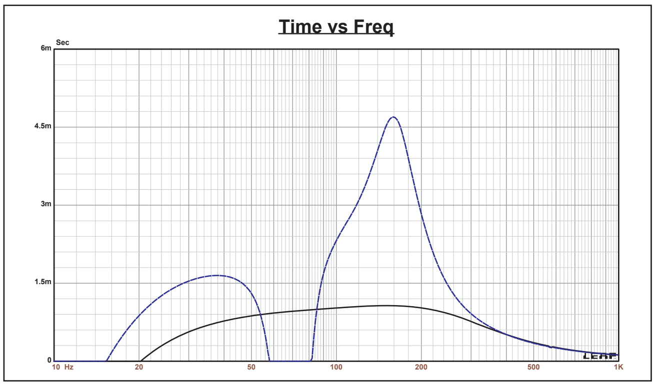

Figure 3: Group delay curves for the 2.83 V curves shown in Figure 2

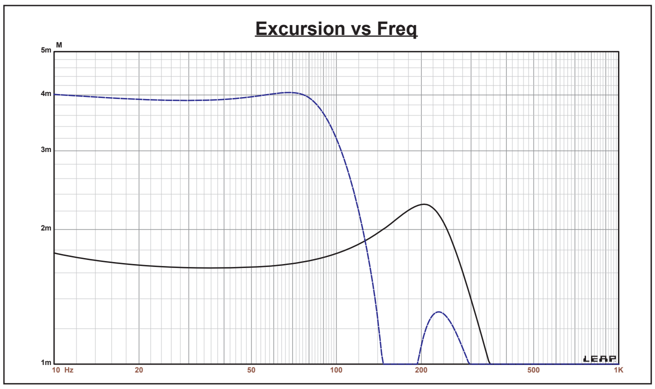

Figure 4: Cone excursion curves for the 15 V curves shown in Figure 2

Figure 1 shows the 1 V free-air impedance curve. **Table 1** compares the LEAP 5 LTD, the TSL data, and the factory parameters for both of the Dayton Audio DMA58-4 samples.

LEAP TSL/LTD parameter calculation results for the DMA58-4 were decidedly similar to the factory data. There was a variation in the sensitivity numbers, but mine are calculated from the Thiele-Small (T-S) routine, while the Dayton data appears to be a SPL average at some specified bandwidth. As always, I followed my usual protocol and set up computer enclosure simulations using the LEAP LTD parameters for Sample 1. This consisted of a

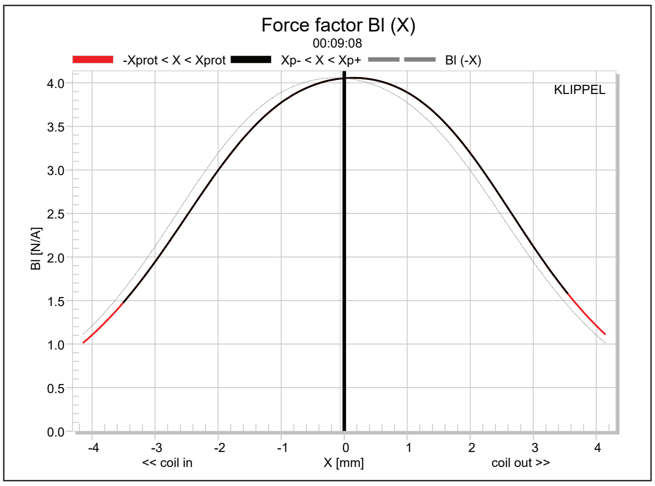

Figure 5: Klippel analyzer Bl(X) curve for the Dayton Audio DMA58

5.2 in^3 Butterworth sealed box with 50% damping material (fiberglass), and an 8.3 in^3 passive radiator incarnation using the data from a Dayton DMA58-4 2” drone radiator. This alignment was tuned to 70 Hz with 15% damping material (fiberglass) in the box.

Figure 2 displays the results for the DMA58-4 in the sealed and box simulations at 2.83 V and at a voltage level sufficiently high enough to increase cone excursion to Xmax + 15% (2.3 mm for the DMA58-4). This produced a F3 frequency of 252 Hz (F6 =191 Hz) with a Qtc = 0.68 for the 5.2 in^3 sealed enclosure and −3 dB = 158 Hz (-6 dB = 145 Hz) for the 8.3 in^3 passive radiator simulation. Increasing the voltage input to the simulations until the maximum linear cone excursion was reached resulted in 97 dB at 20 V for the sealed enclosure simulation and the same 97 dB with the same 10 V input level for the passive enclosure. **Figure 3** shows the 2.83 V group delay curves. **Figure 4** shows the 20/10 V excursion curves). The voltage to the passive radiator simulation was limited to 10 V as the excursion curves rises steeply below 110 Hz. As with any

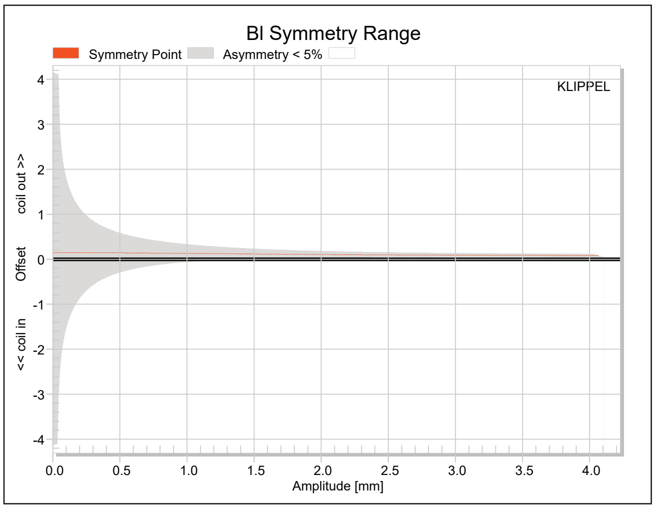

Figure 6: Klippel analyzer Bl symmetry range curve for the Dayton Audio DMA58

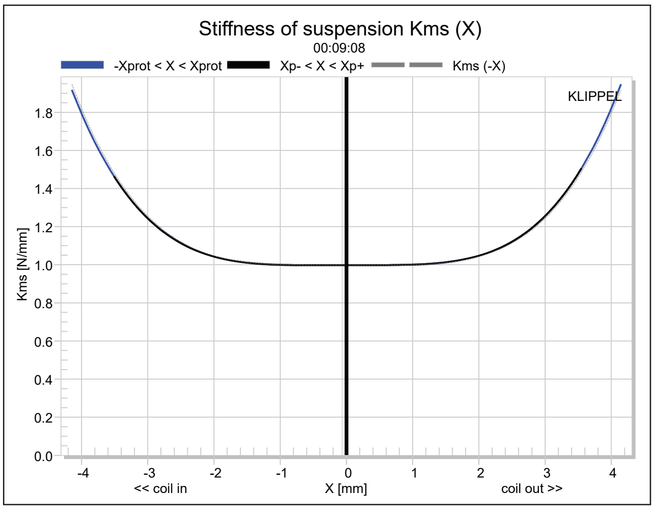

Figure 7: Klippel analyzer mechanical stiffness of suspension Kms(X) curve for the Dayton Audio DMA58

vented or passive radiator enclosure, a high-pass filter is highly desirable and would increase the useful output of the DMA58 substantially.

Klippel analysis for the DMA58-4 produced the Bl(X) and Kms(X) shown in **Figures 5-8**. The Bl(X) curve for the DMA58-4 (see Figure 5) is typical for a short Xmax driver and is very symmetrical with little or no offset. Looking at the Bl symmetry plot (see Figure 6), this curve validates the Bl(X) curve and also shows virtually no offset. The stiffness of suspension Kms (X) curve (see Figure 7) is also very symmetrical, with zero tilt and no offset. Looking at the Kms symmetry range curve (see Figure 8), again there is no offset to consider.

Figure 9 gives the inductance curve Le(X). Inductance will typically increase in the rear direction from the zero rest position, which is what happens here, however, the DMA58 incorporates a copper shorting cap so the inductive swing is very small. Inductance variation for the DMA58-4 is only 0.01 mH to 0.02 mH from the coil-in and coil-out Xmax positions, which is good.

Next I mounted the DMA58-4 in an enclosure that had a 9” × 4” baffle and was filled with damping material (foam). Then, I measured the transducer on- and off-axis from

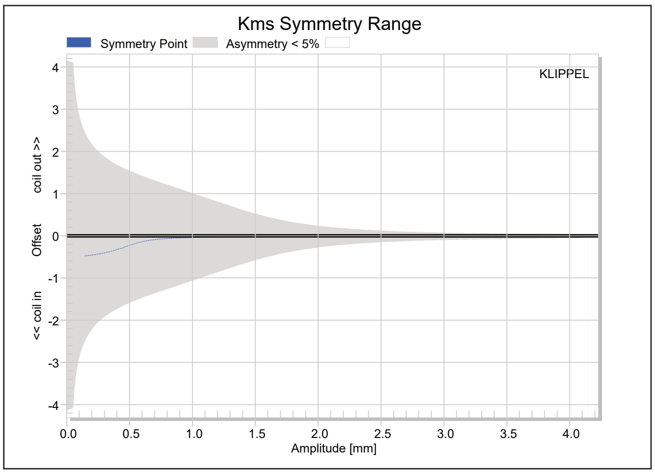

Figure 8: Klippel analyzer Kms symmetry range curve for the Dayton Audio DMA58

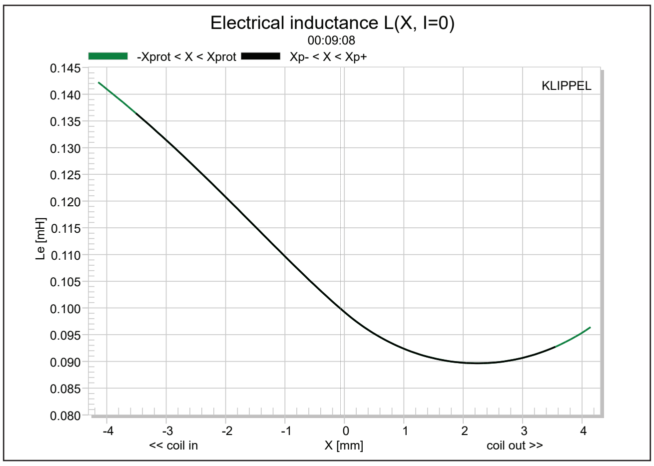

Figure 9: Klippel analyzer L(X) curve for the Dayton Audio DMA58

300 Hz to 40 kHz frequency response at 2.83 V/1 m using the 192 kHz Loudsoft FINE R+D analyzer and the GRAS Sound & Vibration 46BE microphone. **Figure 10** gives the DMA58-4's on-axis response indicating a ±4 dB SPL variation from 300 Hz to 20 kHz with sharp break up mode peaking modes at 21 kHz to 33 kHz.

Figure 11 displays the on- and off-axis frequency response at 0°, 15°, 30°, and 45°. **Figure 12** gives the off-axis curves normalized to the on-axis response, with the Audiomatica CLIO 180° polar plot (measured in 10° increments) depicted in **Figure 13**. The two-sample SPL comparison is illustrated in **Figure 14**, showing the two samples to be matched with 0.5 dB to 0.75 dB, except for a small area centered on 2 kHz.

Next, I employed the Listen, Inc. AudioConnect analyzer

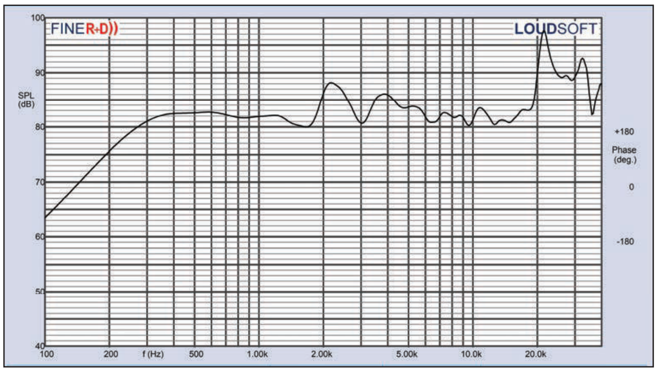

Figure 10: Dayton Audio DMA58 on-axis frequency response

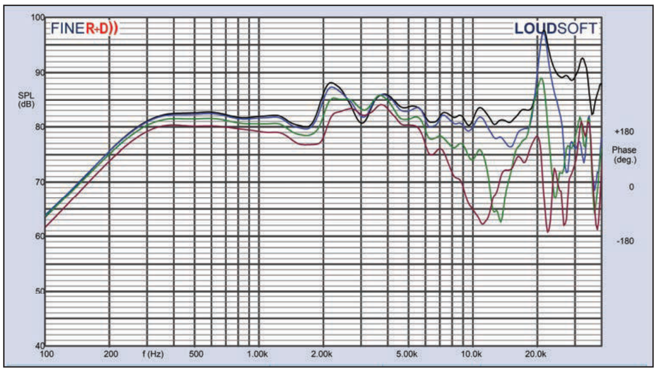

Figure 11: Dayton Audio DMA58 on- and off-axis frequency response (black = 0°, blue = 15°, green = 30°, and purple = 45°)

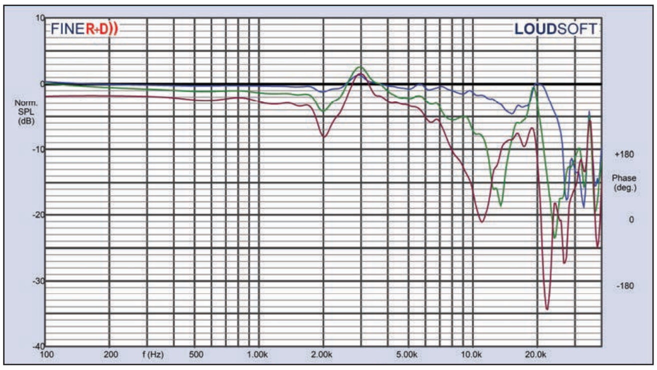

Figure 12: Dayton Audio DMA58 normalized on- and off-axis frequency response (black = 0°, blue = 15°, green = 30°, and purple = 45°)

operating with SoundCheck 17 software along with the Listen 1/4" SCM microphone (courtesy of Listen, Inc.) to measure distortion and generate time-frequency plots. For the distortion measurement, the DMA58-4 was mounted rigidly in free-air, and the SPL set to 94 dB at 1 m (9.86 V), using a pink noise stimulus. The distortion was measured

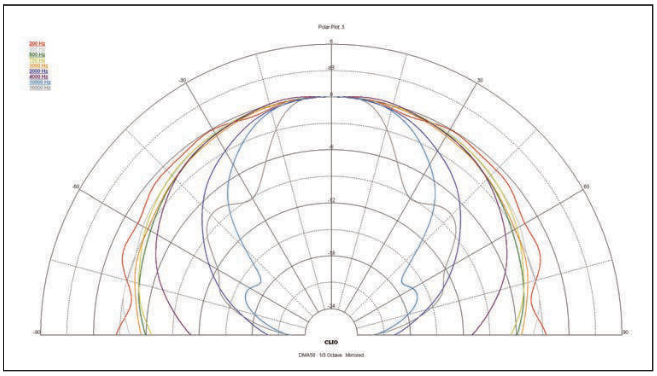

Figure 13: Dayton Audio DMA58 180° horizontal plane CLIO polar plot (in 10° increments)

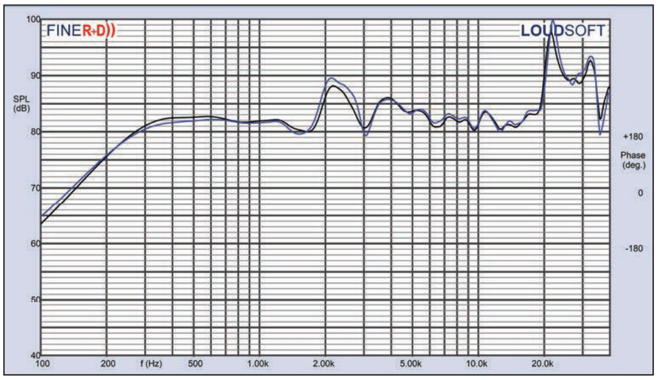

Figure 14: Dayton Audio DMA58 two-sample SPL comparison

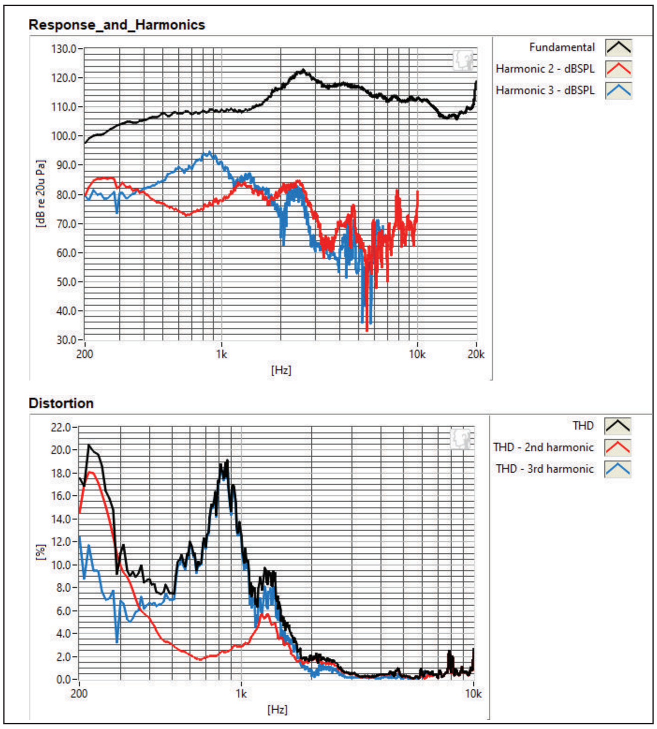

Figure 15: Dayton Audio DMA58 SoundCheck distortion plot

Solen Fast Capacitors™ & Solen Perfect Layer Inductors, often imitated, sometimes copied - even counterfeited - yet never equaled.

SOLEN CAPACITORS
Metallized Polypropylene Flim Fast Capacitors™
-First to use the "Fast Capacitors"™
-First to use bi-axially oriented metabolized polypropylene film
-Lowest dissipation factor, lowest dielectric absorption
-Widest range of values, from 0.01uf to 330uf
-Widest range of voltages, from 250Vdc to 630Vdc
Metallized Teflon™ Film - 0.22uf to 10uf, 1300Vdc
Silver Metallized Polypropylene Film - 0.10uf to 56uf, 700Vdc
Teflon™ Film & Foil - 0.033uf to 0.82uf, 1000Vdc
Polypropylene Film & Tin Foil - 0.01uf to 8.2uf, 100Vdc to 1200Vdc
Metallized Polypropylene Can Type - 22uf, 33uf, 51uf & 100uf, 630Vdc
Metallized Polyester Film - 1.0uf to 47uf, 160Vdc
Non-Polar Electrolytic .5% DF - 10uf to 330uf, 100Vdc
Polarized Electrolytic - .33uf to 33000uf, 63Vdc to 450Vdc

SOLEN INDUCTORS
Perfect Layer Hexagonal Winding Air Core
-First to use Perfect Layer Hexagonal winding technique
-First to use Hepta-Litz seven strand insulated wire
-First to use H49-Litz forty-nine strand insulated wire
-Zero distortion air core, lowest dc resistance
-Widest range of values 0.05mH to 85mH
-Wide range of wire diameters, from 0.8mm (20awg) to 3.1mm (8awg)

SOLEN RESISTORS
Wire wound 10w 5% - 0.5 ohm to 82 ohm
Metal Oxide Link 10w 5% non inductive - 1 ohm to 47 ohm
AchrOhmiC 16w 2% MIL Spec non inductive - 0.5 ohm to 82 ohm

SOLEN TUBES
-Electro Harmonix -Genalex Gold Lion
-Mullard -Sovtek -Tesla JJ -Tung-Sol

MULTIPLE BRANDS OF LOUDSPEAKER DRIVER UNITS
ALL THE ACCESSORIES YOU NEED

Contact us
3940 Wilfrid Laurier Blvd.,
St-Hubert, QC, J3Y 6T1, Canada
Tel: 450.656.2759
Fax: 450.443.4949
Email: solen@solen.ca
Web: www.solen.ca
Find us on: facebook

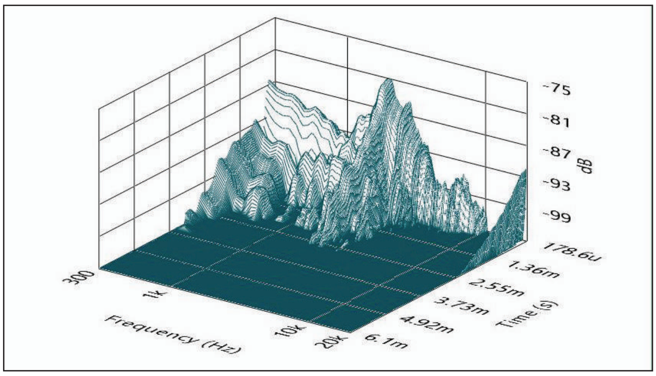

Figure 16: Dayton Audio DMA58 woofer SoundCheck CSD waterfall plot

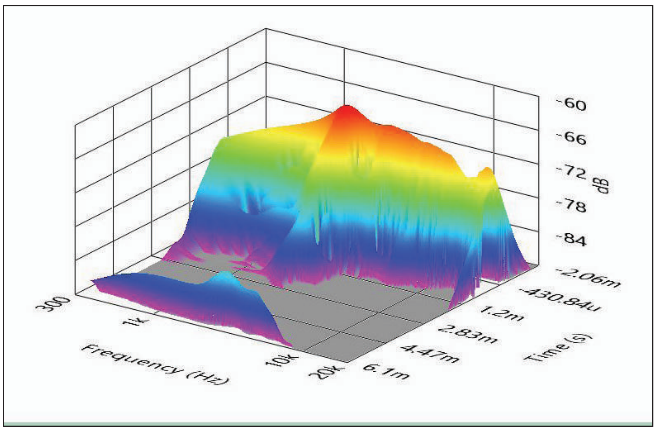

Figure 17: Dayton Audio DMA58 SoundCheck Wigner-Ville plot

with the microphone placed 10 cm from the dust cap. This produced the distortion curves shown in **Figure 15**.

I then used SoundCheck to get a 2.83 V/1 m impulse response for this driver and imported the data into Listen's SoundMap Time/Frequency software. The resulting cumulative spectral decay (CSD) waterfall plot is shown in **Figure 16**. The Wigner-Ville plot (used for its better low-frequency performance) is shown in **Figure 17**.

The performance of the DMA58 is quite good for this small of a driver, and should be quite effective in array applications. For more information about this and other Dayton Audio transducers, visit www.daytonaudio.com. ***VC***

Submit Samples to Test Bench

Test Bench is an open forum for OEM driver manufacturers in the loudspeaker industry and all OEMs are invited to submit samples to *Voice Coil* for inclusion in the monthly Test Bench column.

Send samples in pairs and addressed to:

Vance Dickason Consulting
333 S. State St., #152
Lake Oswego, OR 97034
(503-557-0427)
vdconsult@comcast.net

All samples must include any published data on the product, patent information, or any special information necessary to explain the functioning of the transducer. This should include details regarding the various materials used to construct the transducer. For woofers and midrange drivers, please include the voice coil height, gap height, RMS power handling, and physically measured Mmd (complete cone assembly including the cone, surround, spider, and voice coil with 50% of the spider, surround and lead wires removed).


Custom Installation Speakers
Car Audio Speakers
Loudspeaker Drivers
Home Theater Systems
Active Speakers
Speaker Cabinets
HiVi - hear the difference

Test Bench

A Pro Sound Transducer from BMS

By Vance Dickason

The compression driver being characterized this month came from the highly respected German Pro Sound OEM manufacturer BMS, the 1″ 5530ND (see **Photo 1**). This transducer is being introduced by BMS as a new generation of compression drivers offering a compact physical package that is only 72 mm in diameter, ultra-low intermodulation distortion ring diaphragm, and very high efficiency.

Designed for use with 1″ throat horns, the 5530ND has a 25.4 mm (1″) throat diameter driven by a 44 mm (1.75″) diameter two-layer sandwich voice coil wound on both the inside and outside of the Kapton former with copper clad aluminum wire (CCAW) driving a single-piece polyester diaphragm and surround.

Other features include a FEA-optimized neodymium magnet motor structure, a continuous AES-rated power handling of 80 W with a peak power handling of 450 W, a 1 kHz recommended crossover frequency, and 1 W/1 m 117 dB sensitivity measured in a plane wave tube, and 113 dB measured with a 90° × 75° horn.

This patented design's designated applications include use in a high output point source, in high output line arrays, and in high output beam steering arrays. In an array with the 5530ND drivers spaced 72 mm apart, the crossover frequency can be dropped to 850 Hz, which is quite low for a 1″ compression driver. Since this is a recently released design for BMS, there isn't a BMS 1″ horn available as yet. Given this, I used a Faital Pro LTH102 cast-aluminum Elliptical Tractrix 1″ horn with a 60° × 50° coverage pattern and a recommended crossover frequency of 1 kHz—perfect for the BMS 5530ND compression driver.

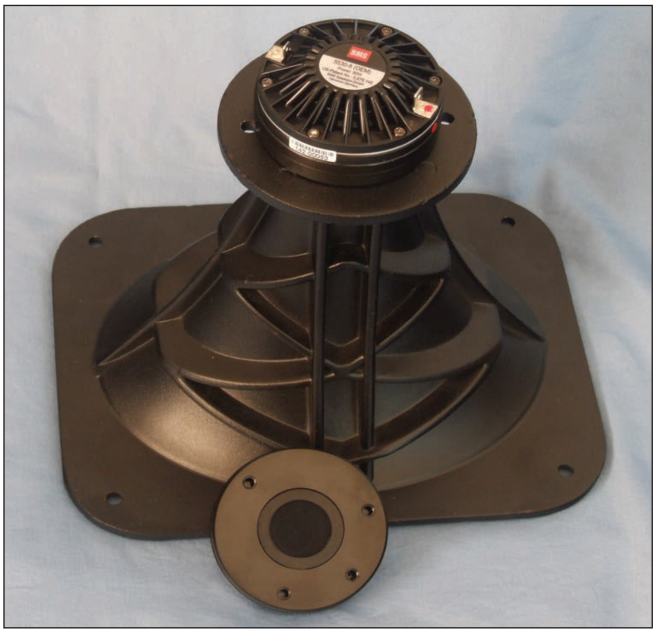

Photo 1: The BMS 5530ND pro sound transducer

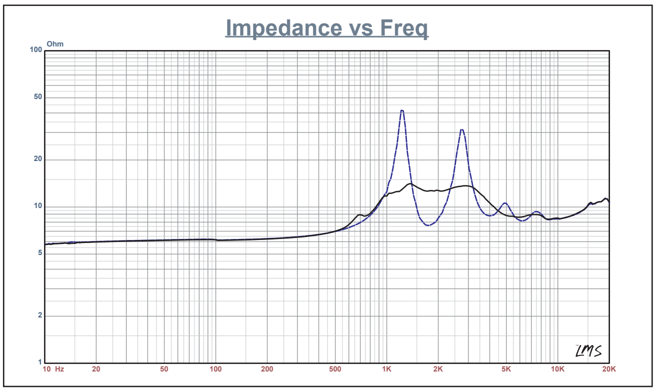

Figure 1: BMS 5530ND free-air impedance plot

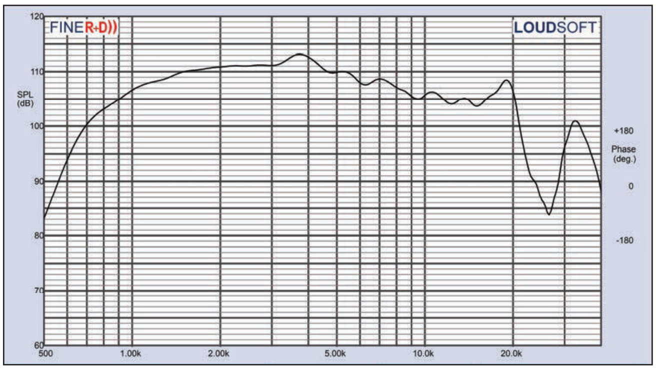

Figure 2: BMS 5530ND on-axis frequency response

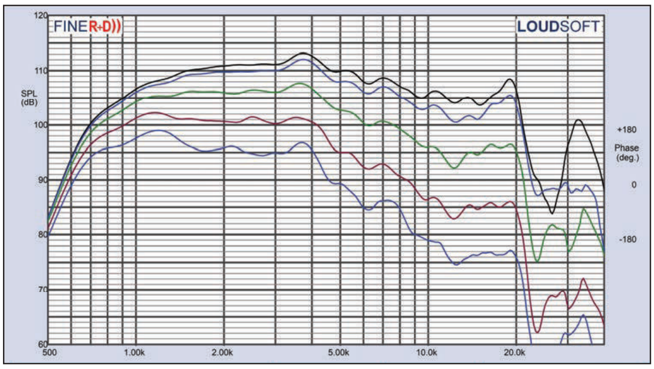

Figure 3: BMS 5530ND horizontal on- and off-axis frequency response (0° = black; 15° = blue; 30° = green; 45° = purple; and 60° = blue)

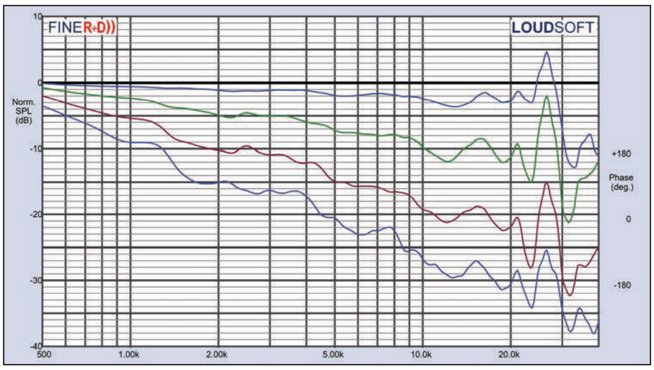

Figure 4: BMS 5530ND normalized horizontal on- and off-axis frequency response (0° = black; 15° = blue; 30° = green; 45° = purple; and 60° = blue)

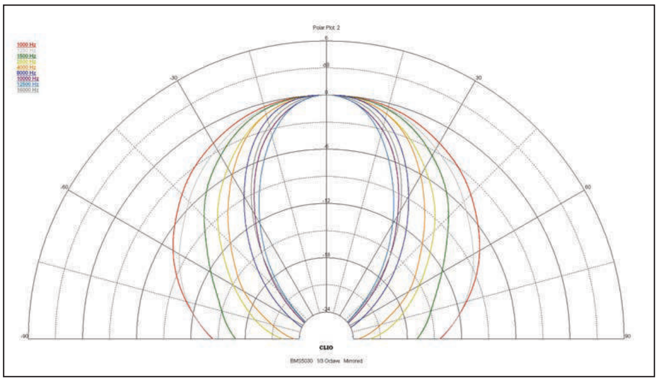

Figure 5: BMS 5530ND horizontal plane polar plot (in 10° increments)

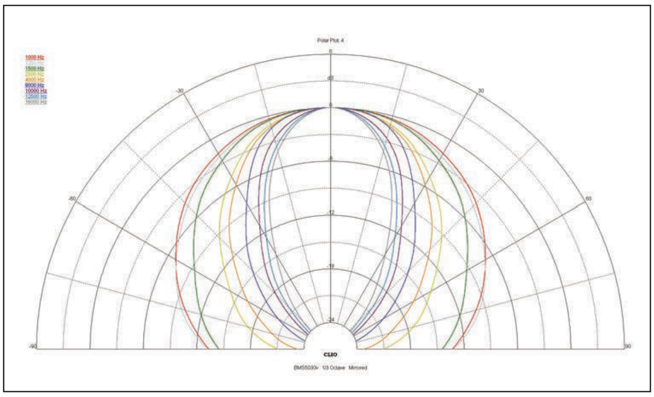

Figure 6: BMS 5530ND 0°-180° vertical plane polar plot (in 10° increments)

I began testing by using the LinearX LMS analyzer to produce the 300-point stepped sine wave impedance plot shown in **Figure 1**, with the solid black curve showing the 5530ND mounted on the LTH102 horn and the dashed blue curve representing the compression driver without the horn. With a nominal 8 Ω impedance (the 5530 is also available in 16 Ω), the 5530ND had 6.18 Ω DCR (Re), with a minimum impedance mounted on the LTH102 horn of 8.36 Ω and at 8.7 kHz.

For the next measurements, I free-air mounted the BMS 5530ND/LTH102 combination without an enclosure and measured both the horizontal on and off axis at 2.0 V/0.5 m (normalized to 2.83 V/1 m) from 0° on-axis to 60° off-axis using the Loudsoft FINE R+D analyzer and GRAS 46BE microphone (supplied courtesy of Loudsoft and GRAS Sound & Vibration). Note: I only measured the horizontal

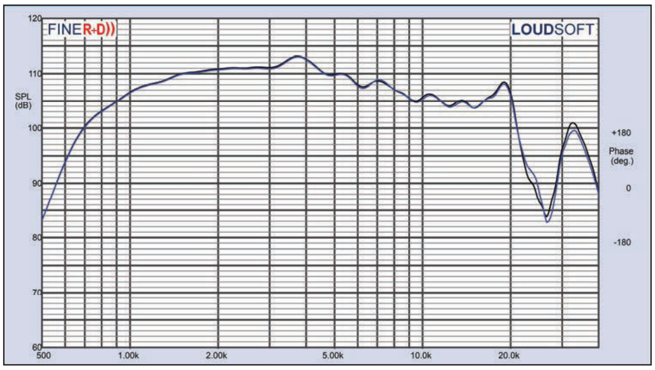

Figure 7: BMS 5530ND two-sample SPL comparison

plane because the LTH102 has appeared in Test Bench reviews previously, however, if you are curious about the LTH102's vertical response, I included a vertical polar plot.

Figure 2 shows the on-axis frequency response of the compression driver/horn, which is relatively smooth with no major anomalies from the 1 kHz recommended crossover frequency to about 20 kHz, with the typical downward sloping response of an elliptical horn.

Figure 3 shows the 0° to 60° on- and off-axis response in the horizontal plane. **Figure 4** shows the normalized horizontal plane response. **Figure 5** shows the 180° horizontal plane polar plot (in 10° increments with 1/3 octave smoothing applied), which was generated by the CLIO Pocket analyzer and accompanying microphone (courtesy of Audiomatica SRL). **Figure 6** shows the CLIO Pocket-generated 180° vertical plane polar plot (also with 10° increments with 1/3 octave smoothing applied). Last, **Figure 7** illustrates the two-sample SPL comparison showing the two BMS 5530ND compression driver samples to be closely matched within 0.25 dB or less throughout their entire operating range.

I again set up the Listen, Inc. AudioConnect analyzer and 1/4" SCM microphone (provided by Listen, Inc.) to measure distortion and generate time-frequency plots. For the distortion measurement, the BMS 5530ND/LTH102 combination was again mounted in free-air in the same manner as was used for the frequency response measurements, and the SPL was set to 104 dB at 1 m (1.26 V, determined by using a pink noise stimulus generator and internal SLM in the SoundCheck 17 software). The distortion was measured with the Listen microphone placed 10 cm from the mouth of the horn. This produced the distortion curves shown in **Figure 8**.

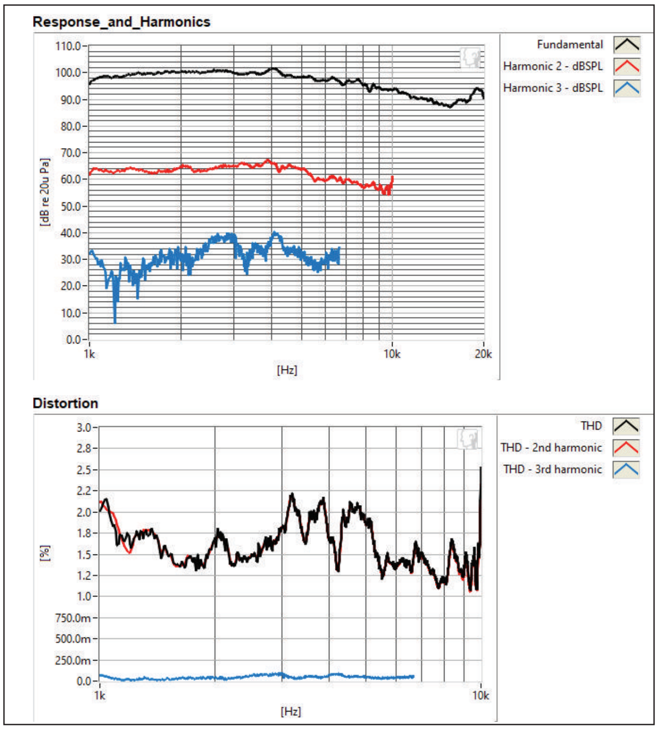

Figure 8: BMS 5530ND SoundCheck distortion plots

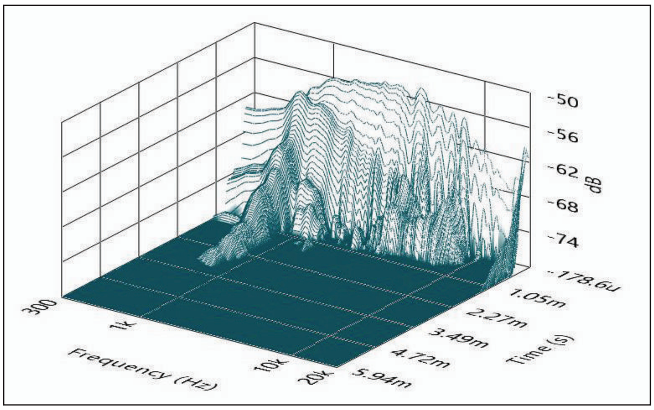

Figure 9: BMS 5530ND SoundCheck CSD waterfall plot

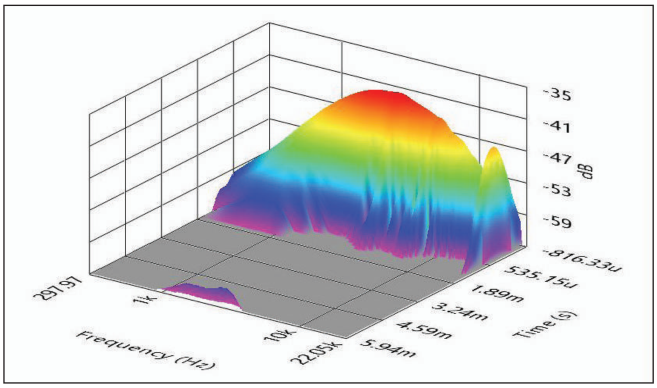

Figure 10: BMS 5530ND SoundCheck Short Time Fourier Transform (STFT) plot

I then set up SoundCheck 17 to generate a 2.83 V/1 m impulse response curve for this driver/horn and imported the data into Listen's SoundMap Time/Frequency software. **Figure 9** shows the resulting cumulative spectral decay (CSD) waterfall plot. **Figure 10** shows the Short Time Fourier Transform (STFT) plot.

When you examine all the data I took on the BMS 5530ND, it's obvious that this is very well-designed product with some appropriate trade-offs resulting in an interesting new choice for a 1" compression driver, especially in arrays. For more on the 5530ND (there is also a screw-in version, the 5531ND), visit www.bmsspeakers.com. ***VC***

Submit Samples to Test Bench

Test Bench is an open forum for OEM driver manufacturers in the loudspeaker industry and all OEMs are invited to submit samples to *Voice Coil* for inclusion in the monthly Test Bench column.

Send samples in pairs and addressed to:

Vance Dickason Consulting
333 S. State St., #152
Lake Oswego, OR 97034
(503-557-0427)
vdconsult@comcast.net

All samples must include any published data on the product, patent information, or any special information necessary to explain the functioning of the transducer. This should include details regarding the various materials used to construct the transducer. For woofers and midrange drivers, please include the voice coil height, gap height, RMS power handling, and physically measured Mmd (complete cone assembly including the cone, surround, spider, and voice coil with 50% of the spider, surround and lead wires removed).

Industry Watch

By Vance Dickason

Sound United Cancels Onkyo/Pioneer Acquisition

Earlier this year, Sound United announced the addition of Pioneer and Onkyo's home audio divisions to the list of brands it owns. Its properties already included Boston Acoustics, Denon, Marantz, and Polk, but the company believed adding those two would allow it to expand its market and release products in more categories. Something must have gone wrong during the acquisition process, though, because Sound United and Onkyo (which also owns Pioneer) called off the deal.

Completion of the acquisition hinged on several conditions, including satisfactory due diligence and securing of committed financing. According to a statement released by Sound United, the companies decided not to push through with the agreement after determining that they couldn't fulfill all those conditions and close the deal by the November 30, 2019 deadline. This from Sound United:

"As was shared at the time, the completion of the transaction was subject to several conditions, including the finalization of all definitive agreements, completion of satisfactory due diligence, securing of committed financing and various other required approvals.

At this point, we have mutually agreed that it is in the best interest of both organizations to terminate the proposed acquisition. After months of rigorous work and negotiations, it became apparent that all of the necessary closing conditions could not be satisfactorily achieved.

Sound United remains dedicated to our mission of Bringing Joy to the World Through Sound. We will continue to pursue this mission through organic growth with our existing brands and through opportunistic acquisitions which allow us to better serve the consumer."

Onkyo reportedly decided to dedicate its attention to running its home AV business instead of focusing on B2B products and services like it wanted to do after selling to Sound United. Forbes says the Japanese company still believes there's value in the deal, though, and is open to discussions, if conditions change.

Audio Precision Launches the APx500 Flex Audio Analyzer

Audio Precision (AP) has officially released the APx500 Flex audio analyzer, enabling the use of APx audio measurement software with ASIO-capable third-party audio interfaces and sound cards. With the introduction of APx500 Flex, manufacturers can cost-effectively deploy the measurement capabilities, flexibility, and quality of APx software to their production lines.

The APx500 Flex audio analyzer is Audio Precision's APx500 measurement software operating independently of an AP hardware analyzer, with licensing controlled by an APx500 Flex Key. In lieu of a purpose-built analyzer, Flex can be paired with ASIO-capable third-party audio interfaces to create a cost-effective solution for a variety of acoustic and electrical test applications.

Measurement scenarios where hardware performance requirements are secondary to test system price (production line test of speakers, headphones, and microphones are ideal candidates for Flex). APx500 Flex enables users to leverage test development done in the R&D cycle through the ability to import project and template files developed for AP hardware analyzers, thereby reducing test development time and maintaining consistency in test methodology across the organization. APx500 Flex also makes for a powerful, portable audio measurement system for application engineers and QA technicians on the go.

APx500 Flex is being introduced in conjunction with the release of APx500 software version 5.0.2, which provides improved ASIO support, including the calibration of inputs and outputs in V, Pa, and Fs, automatic or manual delay compensation for compliant ASIO interfaces, and support for generator trigger, and acoustic and impedance measurements.

Any ASIO-enabled audio interface should suffice with APx500 Flex. However, AP has verified the compatibility of three different audio interfaces—the RME Fireface UC, Lynx Aurora (n), and Lynx E22—and configuration templates for these devices are included in APx500 software version 5.0.2. Each of these verified compatible interfaces offer quality analog I/O (<90 dB THD+N, 192 kHz SNR) and stable drivers with consistent delay. Contact the manufacturers or their authorized resellers for more information. For more information about the new APx500 Flex, visit www.ap.com.

PCB Piezotronics Develops New Microphone Handbook

PCB Piezotronics, Inc. has released a new microphone handbook for use by intermediate level acoustic engineers. The PCB team of acoustic experts and mechanical, industrial, and electrical engineers shared more than 35 years of their

collective microphone design and manufacturing experience in the new microphone handbook. Sample topics include:

- Sensor selection, including prepolarized (0 V) and traditional externally polarized (200 V) designs
- Detailed comparison of in-the-field versus factory calibrations
- Proper handling and maintenance tips for test and measurement microphones
- Information on the most common industry standards

To get technical information in a user-friendly, easy-to-read format, download your free copy of the *PCB Piezotronic Microphone Handbook* from: https://bit.ly/MicrophoneHandbook.

Prism Sound Test & Measurement Changes Its Name to Spectral Measurement

Prism Sound's Test & Measurement division has re-launched itself specializing exclusively in audio test & measurement solutions and trading under the new name of Spectral Measurement. Prism Media Products, Ltd., the company behind the innovative dScope Series III Audio Analyzer, will now focus exclusively on developing new audio test and measurement solutions. The move follows the recent announcement that Prism Sound's Music and Post Production division, which incorporates SADiE, has joined forces with the US-based Tracktion Software Corp. and is now operating under the umbrella of Audio Squadron.

ALTI
Audio & Loudspeaker
Technologies International

ALTI Update

While the 2020 Audio & Loudspeaker Technologies International (ALTI) Expo set for June 14–15 might seem far off, planning has been underway for months, and some very exciting things are in the works.

System Builders Workshop will expand on its 2019 success, making it an immersive 2+ day workshop. Module 1 of the workshop is a full day on the first day ALTI-EXPO 2020 and will focus upon the design, modeling, and building of a speaker and enclosure along with performance testing.

Module 2 will be a half day set for the second day of the expo and will see participants adding an amplifier with Bluetooth to the system along with the appropriate modeling and testing. Module 3 will take place at InfoComm, which is scheduled to start immediately after the ALTI-EXPO and participants will add DSP along with all of the proper modeling, testing, and learning how to best use DSP. At the end of this technical workshop series, participants will have a fully functional wireless speaker to take home with them.

"This is the start of the growing cooperation agreement with our friends at InfoComm. But there is more! What good is a great 'new product' without a plan to produce, market, and sell it profitably? The Business Builders Workshop (BBW) will be an executive-level deep dive into recognizing opportunities and evaluating markets and risks for best ROI. Then the workshop will delve into brand development and creating a compelling reason to engage. Taught by Adrian Weidmann and others, this is an extended workshop on Day 2 of the ALTI-EXPO," said Barry Vogel, ALTI executive director.

At InfoComm, on a main stage, Participant Teams at BBW will present their new "product" to actual buyers of this type of product in a "Shark Tank" game show kind of environment that will be called the Tiger Pit. Details can be found on the ALTI website: https://almaint.org/elementor-5181.

The "Call for Content" is also now available to participate in ALTI's acclaimed education program. Get your form at: https://almaint.org/alti-expo-2020-content. Early Exhibitor discounts are in place until December 30. 2019.

The best locations go first, so claim your spot at: https://almaint.org/elementor-5181. Keep checking the website for updates, or sign up for the free newsletter for updates at: https://almaint.org/contact-us. ***VC***


Ch1
Ch2
0.003102 %
0.003036 %
0.0001
0.001
0.01
0.1
1
10
100
THD+N Ratio (%)
APx500 Flex Key